



The tectonic framework of the Alto Guaporé Belt, Amazonian Craton, Brazil, revealed by the integration of airborne geophysics, and geological and geochronological data

Carlos Eduardo Santos de Oliveira^{1,2*}, Adalene Moreira Silva¹, Jaime Estevão Scandola³

¹Institute of Geosciences, Universidade de Brasília (UnB), Asa Norte - Brasília, DF, Brazil, CEP: 70.910-900

²Geological Survey of Brazil, Av. Lauro Sodré, 2561, São Sebastião, Porto Velho-RO, Brazil, CEP: 76.801-581

³Geological Survey of Brazil, SBN Quadra 02, Bloco H - Asa Norte - Edifício Central Brasília Brasília, DF, Brazil, CEP: 70.040-904

Abstract

The Alto Guaporé Belt represents a key component in the investigation of the geological history and reconstruction of the SW Amazonian Craton. Airborne geophysical, isotopic and geochronological data integrated with field data have provided new insight into the tectonic framework of this terrane. More than 90,000-line kilometers of airborne geophysical data, including magnetic and gamma-spectrometry data, obtained over 43,018 square kilometers in the southeastern part of Rondônia and northwestern limit of Mato Grosso states between 2005 and 2006. Aeromagnetic data allowed the generation of geophysical maps, including the total magnetic intensity, the first order derivative, and the analytic signal amplitude, which enabled the identification of terrane limits, structural pattern and geometry of magnetic bodies. The integration of these products resulted in qualitative models of magnetic and structural domains highlighting and characterizing the three deformation events. The pseudo-gravity map enhanced the deep structures, and shows clear discrimination of deep sources between the Alto Guaporé Belt and the Jauru Terrane. This relation is not easily understood when a conventional analysis of magnetic data is performed. The airborne gamma-ray spectrometry data showed areas of radioelements concentration and dispersion, improving the geologic mapping for the definition of geologic contacts, intrusive bodies and the overlap of areas with sedimentary covers and regolith material. The geological, geochronological U-Pb and isotopic Sm-Nd data helped constrain the geodynamic evolution for this portion of the Amazonian Craton. The geodynamic history and geologic architecture are important parameters for the definition of mineral systems and mineral exploration targeting models at regional and local scales.

Article Information

Publication type: Research Papers
Received 26 November 2021
Accepted 5 April 2022
Online pub. 11 April 2022
Editor: David L. Castro

Keywords:
Amazonian Craton,
Alto Guaporé Belt,
Airborne Geophysics,
U-Pb,
Sm-Nd

*Corresponding author
Carlos Eduardo Santos de Oliveira
carlos.oliveira@cprm.gov.br

1. Introduction

The southeastern Amazonian Craton in Rondônia is poorly exposed, with a well-developed regolith and represents a key region with wide and unexplored gold and nickel mineral potential. The knowledge of mineral occurrences is limited to different associations, like the gold mine of Zé Goiano, the Serra Céu Azul Complex (Cu-Ni and PGE) (Romanini 1997, 2000), Morro do Leme and Morro-Sem-Boné (Ni-Cu-Co + PGE) (Nunes 2000).

Rizzotto and Hartmann (2012) defined an incomplete ophiolite sequence in the mafic-ultramafic Trincheira Complex, and consequently, the suture zone between the Amazonian protocraton and the Paragua Craton, emphasizing the interest

in the mineral potential of the southeastern part of Rondônia. However, a large part of the region is covered by Cenozoic sediments of the Guaporé river basin to the south, and by Phanerozoic sedimentary rocks of the Parecis Basin to the north, restricting the exposed basement area to approximately 4,000 km². In addition, the absence of continuous outcrop, thick weathering profile and the level of rocks alteration masks the relations among the several tectono-stratigraphic units and complicates geological mapping.

The use of airborne geophysical data aided in the structural framework interpretation of the region based on derivative products from magnetic anomalies and images of K, eTh and eU and their ratios calculated from airborne gamma-ray spectrometry data. Gravity data indicated the



deep features of the tectonic architecture framework. The integrated interpretation of these data contributes to the geological mapping and mineral exploration, especially in tropical terranes with few outcrops. Integration of airborne geophysical, geological and geochemical data in GIS enables the definition of favorable zones to host mineralization on a regional scale (e.g., Jaques et al. 1997; Gunn et al. 1997a, b).

Airborne geophysical measurements complement traditional mapping, allowing the regions to be imagined in two or three dimensions (Milligan and Gunn 1997; Stewart and Betts 2010; Metelka et al. 2011). Large scale geological bodies and the area structural framework were identified in the southeast Rondônia and NW Mato Grosso through the analysis and interpretation of airborne magnetic and gamma-ray spectrometry datasets and the combination with geological, structural and geochronological data in order to improve the understanding of the tectonic framework.

2. Amazonian Craton

The Amazonian Craton, one of the largest and least known Precambrian areas in the world, is one of the main tectonic units of South America (5,600,000 km²). The Amazonian Craton is separated from the Andean orogenic belt by an extensive Cenozoic cover (e.g., Colombian and Venezuelan plains, Paraguayan-Bolivian Chaco), which makes the definition of its western edge difficult. Its extension to the west, below the Cenozoic cover, is suggested by Mesoproterozoic basement inliers in the Eastern Ridge, such as Garzón and Santa Marta (Kroonenberg 1982; Priem et al. 1989). In Brazil, the Amazonian Craton, with an approximate area of 4,400,000 km², bordered on the east by the Baixo Araguaia Group, on the south and southeast by the Alto Paraguai, Cuiabá and Corumbá groups, and by rocks originated from the Brasiliano Orogenic Cycle (900-540 Ma, Pimentel and Fuck 1992). In this case, the concept of craton applies to the rocks formed before that orogenic cycle, constituting the stabilized area in pre-Brasiliano periods. The craton is also covered by Phanerozoic basins to the east (Parnaíba), south (Xingu and Alto Tapajós), southwest (Parecis), west (Solimões), north (Tacutu), and central area (Amazonas).

The southwestern part of the Amazonian Craton (Fig. 1), which is the target of this work, carries the polycyclic geotectonic evolution record with basement originating from 1.82 Ga and resulting from successive episodes of magmatism, metamorphism, sedimentation and deformation (Scandolara and Amorim 1999). Three geochronological provinces (Cordani et al. 1979; Litherland et al. 1989; Teixeira et al. 1989; Tassinari and Macambira 1999) comprise the geotectonic framework of the SW Amazonian Craton: Rio Negro-Juruena (1800-1550 Ma), Rondonian-San Ignacio (1450-1250 Ma) and Sunsás (1300-1000 Ma). The current geotectonic/geochronological model is based mainly on isotopic Rb-Sr data, with well know limitations in poly-deformed, poly-metamorphosed, or highly metamorphosed areas, where the system can be easily reopened. The geochronological provinces received tectonic connotations, according to a dynamic model of mobile belts type (Cordani and Brito Neves 1982; Litherland et al. 1986; Teixeira et al. 1989; Tassinari 1981; Tassinari et al. 1984, 1996, 2000). For these authors, the mobile belts would develop in parallel during the Mesoproterozoic, from an older core, the Central Amazônia

Province, with age progressively younger in a SW direction of the craton. New geochronological data (conventional, U-Pb, LA-ICP-MS and SHRIMP), reinterpretation of isotopic Sm-Nd values and insertion of information coming from field work, led to a new understanding about the subdivision and evolution of the Amazonian Craton in the Precambrian, with the definition of seven geological provinces (Santos et al. 2000). According to these authors, the SW of the Amazonian Craton consists of only two geological provinces: Rondônia-Juruena (1810-1520 Ma, Ouro Preto orogenesis) and Sunsás (1450-990 Ma, Candeias and Nova Brasilândia orogenesis), built by accretionary/collisional and collisional events respectively.

2.1 Alto Guaporé Belt

The study area (Fig. 1) is located in the NNW border of the Jauru Terrane (Saes and Cesar 1996) and includes almost all the Alto Guaporé Belt (Rizzotto and Hartmann 2012), within the Rondonian/San Ignacio Province (Teixeira and Tassinari 1984; Litherland et al. 1986). The stratigraphic organization of the area under study based on that presented on the Geological Map of Rondônia (Scandolara et al. 1999; Quadros and Rizzotto 2007), with adjustments proposed by Rizzotto (2010). In this region, the following units occur (Fig. 2): (1) Rio Galera Complex; (2) Pindaituba Intrusive Suite; (3) Trincheira Mafic-Ultramafic Complex; (4) Colorado Complex; (5) Syn- to late- tectonic mafic and ultramafic bodies; (6) Syn- to late- tectonic granites of the Igarapé Enganado and Cerejeiras Intrusive Suites; (7) Syn- to post- tectonic granites of the Alto Escondido Intrusive Suite; (8) Paleozoic covers of the Corumbiara Formation and the Parecis Group; and (9) Cenozoic covers of the Guaporé Formation and associated sedimentary covers.

2.1.1. Rio Galera Complex

The Rio Galera Complex consists of biotite-muscovite schists, biotite gneiss, hornblende-biotite gneiss, diopside-hornblende gneiss, sillimanite-quartz schists and hornblende amphibolite. The ⁴⁰Ar/³⁹Ar ages of 1208 ± 3 Ma and 1165 ± 5 Ma in amphibolites suggest a thermal overprint in the late Mesoproterozoic (Ruiz 2005; Tohver et al. 2005, 2006).

2.1.2. Pindaituba Intrusive Suite

The suite represents a set of intrusions within the supracrustal and orthogneiss rocks of the Jauru Domain (Ruiz 2005). The Pindaituba Suite is formed by the Praia Alta and Rio Piolho granites and occurs as elongated batholiths with a N20°-40°W direction, varying in composition from tonalite to syenogranite. Ruiz (2005) used ID TIMS U-Pb analysis of zircon, to determine crystallization ages of 1423 ± 11 Ma.

2.1.3. Trincheira Mafic-ultramafic Complex

The Trincheira Mafic-ultramafic Complex is the main unit of the Alto Guaporé Belt and characterized by an association of mafic-ultramafic rocks containing gabbro, tremolite, hornblendite, and gabbronorite, partly metamorphosed (Pinto Filho et al. 1977; Romanini 2000).

Due to the geological complexity, Rizzotto and Hartmann (2012) divided it into three sub-units: a) lower unit – cumulate

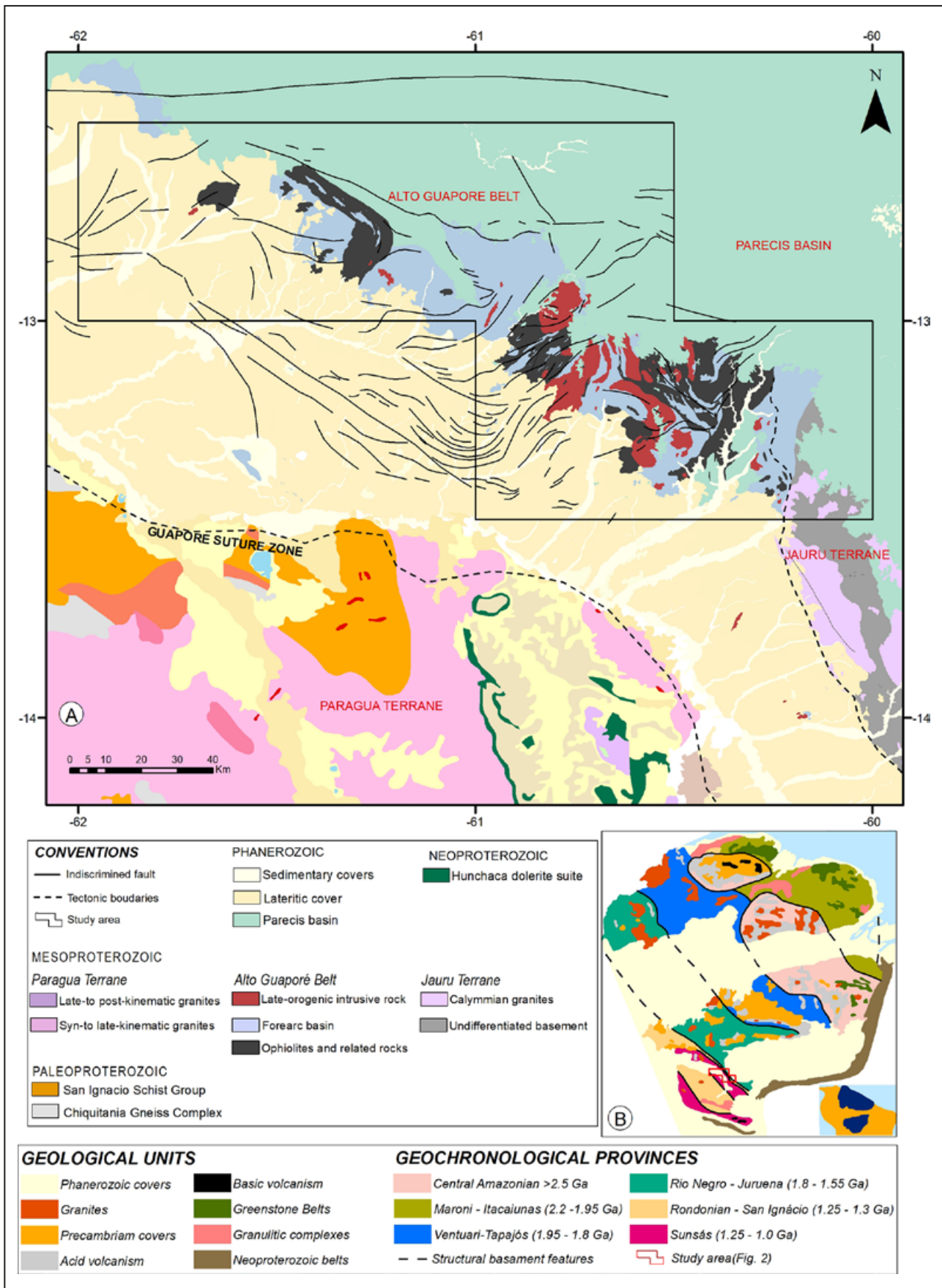


FIGURE 1: (A) Simplified geological map of the southwest of the Amazonian Craton, with approximate limits of the main terranes, belts and mobile belt (Adapted from Schobbenhaus 2001; Rizzotto and Hartmann 2012); and (B) subdivision of the six geochronological provinces according to Tassinari et al. (1996) and Tassinari and Macambira (1999).

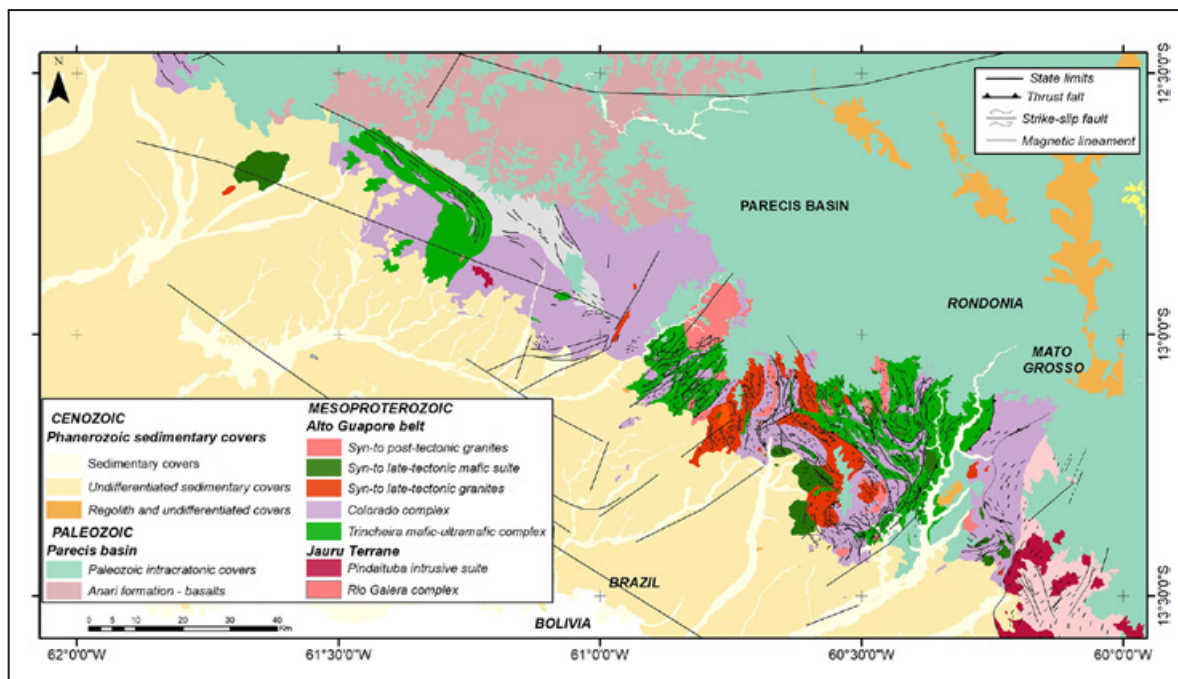


FIGURE 2: Simplified geological map of the area of study in the southeast of the state of Rondônia and SW of Mato Grosso (Adapted from Scandolaro et al. 1999; Quadros and Rizzotto 2007; Rizzotto 2010).

mafic-ultramafic rocks (granulite facies) olivine pyroxene protoliths, bronzitite and websterite; b) intermediate unit – banded amphibolites, with norite, gabbronorite, gabbro, anorthosite gabbro-anorthosite and rare plagiogranite protoliths (amphibolite facies); c) upper unit - fine-grained amphibolite, massive and pillowed basalt with alternation of metachert (BIF), meta-marl and schist (amphibolite facies).

The contact with other units is tectonic and determined by transpressive faults. The mineralogic characteristics and the protoliths of the different types of rocks that comprise the Trincheira Complex are shown in Table 1.

The geochronological records of the Trincheira Complex show an average $^{40}\text{Ar}/^{39}\text{Ar}$ age of 1319 ± 10 Ma (biotite dated), interpreted as regional metamorphic cooling of the Guaporé Belt (Rizzotto et al. 2002). Data obtained from the ratio $^{207}\text{Pb}/^{206}\text{Pb}$ in zircon from a mafic granulite shows an age of 1447 ± 12 Ma, interpreted as the rock crystallization age (Rizzotto et al. 2013).

TABLE 1 - Mineralogic characteristics and protholith of the main kind of rocks of the mafic-ultramafic Trincheira Complex (Rizzotto and Hartmann 2012)

Lithology	Mineralogy	Protholith
Metabasalt	hornblende+plagioclase+epidote+quartz±magnetite±titanite	Basalt
Amphibolite	mg-hornblende+plagioclase+quartz+epidote±titanite±ilmenite±clorite	Gabbro
Porphyroblastic amphibolite	mg-hornblende+plagioclase+quartz+magnetite±ilmenite±apatite±epidote	Gabbronorite
Metagabbro	plagioclase+clinopyroxene+orthopyroxene+actinolite±ilmenite±titanite	Gabbro
Meta-ultramafic	orthopyroxene±plagioclase±cummingtonite	Pyroxenite
Mafic granulite	clinopyroxene+orthopyroxene+plagioclase±hornblende±ilmenite	Norite

2.1.4. Colorado Complex

The Colorado Complex is a metasedimentary unit composed of paragneiss, pelitic schist, calc-silicate gneiss, para-amphibolite and banded iron formation. Rocks from this unit, together with those of the Trincheira Complex, make up the regional high-grade rocks of the Alto Guaporé Belt (Rizzotto and Hartmann 2012).

Geochronological data obtained from the $^{40}\text{Ar}-^{39}\text{Ar}$ technique on hornblende of two samples of amphibolite showed ages of 1313 ± 4 Ma, 1313 ± 6 Ma, 1312 ± 3 Ma, 1325 ± 3 Ma, 1326 ± 2 Ma, 1330 ± 3 Ma, with an average of 1319 ± 10 , and were interpreted as the period of regional metamorphic cooling (Rizzotto et al. 2002).

The paragneiss (metapsammite unit) yielded ages of upper intercept of 1544 ± 21 Ma (U-Pb method), derived from an igneous source, considered by the authors to be related to the main source of sediments and maximum age of sedimentation. The age 1340 ± 30 Ma, determined from a metamorphic zircon, was interpreted as the metamorphic peak recorded in the Colorado Complex (Rizzotto 2010).

2.1.5. Syn- to late-tectonic mafic intrusive suite

There are three main groups of rocks: ultramafic rocks of the Morro-Sem-Boné and Morro do Leme, Igarapé Hermes mafic-ultramafic and Cidade do Colorado mafic rocks (Rizzotto 2010). The Serra Céu Azul Intrusive Suite is not included in this association; however, the unit contains rocks with a high potential for Cr, Ni, and Cu mineralization (Romanini 2000).

The ultramafic rocks of Morro-Sem-Boné consists of serpentinite in the upper portion, with intercalated silcretes and lateritic siliceous layers. Morro do Leme comprises layered bodies of serpentinitized dunite and peridotites and, in a lesser proportion, hornblendite and tremolitite (Rizzotto

2010). The mafic rocks of Cidade do Colorado unit are, in a general way, represented by layered gabbro and metagabbro, with incipient regional deformation. The mafic-ultramafic Igarapé Hermes rocks consist of coarse-grained metagabbro and hornblendite, and occur in the form of large boulders, in the southeastern part of the study area.

The crystallization age of leucogabbro in the Cidade do Colorado Mafic unit yielded an age of 1352 ± 4 Ma (U-Pb method) (Rizzotto et al. 2002).

2.1.6. Syn-to late tectonic intrusive granites

The rocks of the Igarapé Enganado Intrusive Suite comprise medium to coarse-grained syenogranite, monzogranite, granodiorite and rare tonalite with metaluminous to peraluminous chemical signature. They have a light color and show magmatic flow foliation. The Cerejeiras Intrusive Suite comprises gray and pinkish, coarse-grained, inequigranular to porphyritic granites with a characteristic foliation of magmatic flow. Geochemistry and petrogenesis of this suite are similar to those of the Igarapé Enganado Suite. Rizzotto (2010) analyzed samples of granodiorite, using the U-Pb (SHRIMP) method, and presented a result of 1340 ± 5 Ma, interpreted as the igneous crystallization age. In the same sample, Sm-Nd isotopes analyses supplied TDM model ages from 1.58 to 1.51 Ga.

2.1.7. Syn- to post-tectonic intrusive granites

The granites of the Alto Escondido Suite are homogeneous, leucocratic with gray to pink color, fine-grained, and show incipient magmatic flow fabric (biotite monzogranite and garnet-biotite syenogranite). Dating on a sample of biotite syenogranite was performed, using the U-Pb (SHRIMP) method, and gave an age of 1340 ± 3 Ma, interpreted as the age of crystallization age (Rizzotto 2010). The results of the Sm-Nd method of this sample indicated TDM model ages of 1.51 Ga and $\epsilon_{\text{Nd}}(\text{T})+2,35$ Ga, which suggests a juvenile magmatic source. The second analysis (equigranular syenogranite) supplied an age of 1337 ± 4 Ma, using the U-Pb (SHRIMP) method.

2.1.8. Paleozoic intracratonic covers

The Paleozoic covers include the Corumbiara Formation and the units that make up the Parecis Group. Bahia and Pedreira (1998) and Bahia et al. (2007) studied, the glaciogenic deposits of the Pimenta Bueno Formation and the tectono-sedimentary evolution of the Parecis Basin. The Corumbiara Formation comprises a sedimentary package of conglomerates and immature sandstones, diamictites and carbonates. The Parecis Group, in this area, is represented by several formations, such as Anari (basalt, diabase and microgabbro), Rio Ávila (bimodal sandstones) and Utiariti (quartz-sandstone).

2.1.9. Undifferentiated sedimentary covers

The Cenozoic covers recorded in this region consist of the Guaporé Formation and undifferentiated sedimentary covers and represent a large area, apart from the lateritic cover, distributed all over the study area.

3. Materials and methods

3.1. Airborne geophysical data

The airborne geophysical survey in the southeastern of Rondônia was carried out by the partnership of LASA Engenharia e Prospecções S.A. and Prospectors Aerolevantamentos e Sistemas LTDA., for CPRM/SGB – Geological Survey of Brazil. The airborne geophysical survey was flown during 2005-2006, in the southeastern part of Rondônia state and part of the northwestern limit of Mato Grosso state, covering 93,189.12 km of aeromagnetic and aero-gamma-spectrometric profiles data. The aeromagnetic system used in the aerial survey consisted of a cesium steam sensor located in the rear of the aircraft (stinger type), with a resolution of 0.001 nT. The magnetometric readings were performed every 0.1 second, which is equivalent to a speed of 280 km/h of the aircraft and to approximately 7.8 m ground sampling rate. The gamma-ray spectrometry system used, Exploranium, model GR-820, measured the natural gamma radiations spectrum, discriminating 256 spectral channels. The detecting system consists of two sets of crystals (thallium-activated sodium iodide), two downward-looking, with 1024 cubic inches each (total volume of 2048 cubic inches) and two upward-looking, with 256 cubic inches each (totalizing 512 cubic inches; CPRM 2006). The gamma-ray spectrometry readings were performed each second, representing measures at intervals of approximately 78 m on the surface.

The spacing between the N-S flight lines and the E-W control lines is 0.5 km and 10 km, respectively. The nominal height of flight was fixed at 100 m above the surface. The Sudeste de Rondônia airborne survey has an irregular shape because it includes a border region (Fig. 3).

3.2. Geological Data

The geological and mineral resources maps of Rondônia state (Scandolara et al. 1999; Quadros and Rizzotto 2007), and the maps of the Guaporé Project Pimenteiras (SD.20-X-D) and Vilhena sheets (SD.20-X-B) (Rizzotto 2010; Rizzotto 2014) were used as support for the development of this work. The geological-geophysical integration map (Oliveira et al. 2015), based on the interpretation of aeromagnetic and gamma spectrometric data were considered.

3.3. Geochronological Data

In order to understand the crustal evolution of the Alto Guaporé Belt, isotopic geochemical data, Sm-Nd, U-Pb and Ar-Ar of several researchers (Ruiz 2005; Rizzotto 2010; Rizzotto et al. 2013; Scandolara 2006) were integrated and used as reference for geochronological interpretations.

4. Geophysical Data Processing

The data from the Southeast of Rondônia airborne survey was pre-processed by LASA Engenharia e Prospecções S.A. and Prospectors Aerolevantamentos e Sistemas LTDA. All the procedures data reduction performed by LASA was considered definitive; thus, all the processing carried out was based on the final geophysical information provided. The magnetic information, expressed by the total magnetic

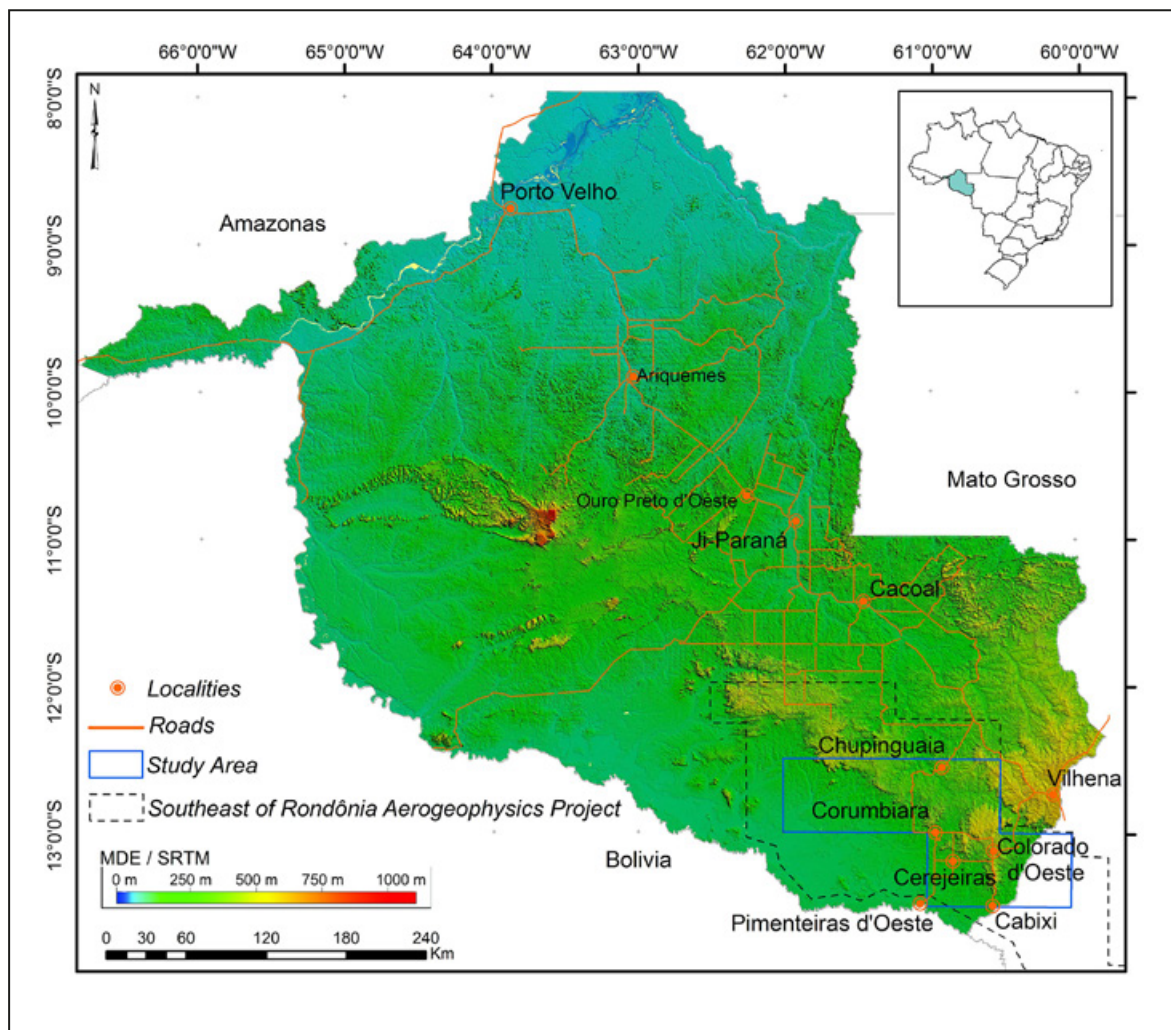


FIGURE 3: Digital elevation model of the state of Rondônia generated from SRTM (Shuttle Radar Topographic Mission) data, indicating the position of the Southeast of Rondônia Airborne Survey (CPRM 2006), study area, and main access roads. Note that the area of the survey is located in the southeast of Rondônia and northwest portion of the state of Mato Grosso.

intensity (TMI), was derived from the total field measured, with the daytime geomagnetic variation correction and the geomagnetic field correction (IGRF) applied. The gamma spectrometric information was provided in separate energetic bands, including the total energy band (channel of the total count) expressed in $\mu\text{R/h}$, the potassium channel, expressed in percentage, and the uranium and thorium channels as part per million. All bands were corrected for dead time energy variations (spectrum stabilization) of the respective levels of background and cosmic radiation. Corrections were also applied for height variations and the Compton Effect. The processing included the leveling and micro leveling of profiles for both datasets (CPRM 2006).

The pre-processing was carried out using the Oasis Montaj TM software (version 9.8.1), in which the original data, obtained from lines (flight lines with N-S direction), was transformed into regular grid format using the bi-directional interpolator, appropriate for data arranged in parallel lines, since it accentuates the tendencies that appear perpendicular to the flight lines. A $125\text{ m} \times 125\text{ m}$ cell size was used to interpolate, representing $1/4$ of the flight line spacing. Gunn et al. (1997b) state that an interpolation routine for magnetic data will only produce realistic interpolation if the unit cells do not exceed 20-25% of the line spacing.

4.1. Magnetometry

The magnetic measurement represents the influence of at least three sources: (i) internal, due to the geomagnetic field, created in the convection cells of the liquid outer core; (ii) external, coming from the influence of several electrical currents established in the ionosphere and (iii) from the crustal magnetic sources (represented by the differences in local concentrations of magnetic geologic material), located at shallow depths below the Curie temperature for magnetite, which is the main source of magnetism for geologic material. The elimination of the influence related to the main magnetic field was performed using an appropriate mathematic model, the IGRF/DGRF (International/Definitive Geomagnetic Reference Field). The removal of the contribution related to external sources was performed by correcting for the daytime geomagnetic variation (Solar Quiet). The final product of these two corrections is the total magnetic intensity (TMI), representing the variations of magnetite concentration in crustal geologic material and features imposed on them.

Several other products were calculated from the TMI, the horizontal derivatives (Dx and Dy), the vertical derivative (1st VD), the total horizontal derivative (THD; Blakely 1996), the

analytic signal (AS; Nabighian 1972), the tilt derivative (TD; Miller and Singh 1994; Salem et al. 2009) and the pseudo-gravity (Baranov 1957) (Fig. 4). Besides these products, TMI upward continued maps of 500 m and 10,000 m were created. The qualitative visual interpretation of these products allowed the generation of the lineaments and magnetic domains.

The TMI represents the magnetic field produced by the magnetic sources present in the study area, without the influence of the Earth's magnetic field. The magnetic anomaly of a finite body invariably includes positive and negative elements created by the dipolar nature of the Earth's magnetic field (Fig. 5-A). The horizontal derivatives (Dx and Dy) (Fedi and Florio 2001; Verduzco et al. 2004; Cooper and Cowan 2006) show the horizontal variations of the TMI and highlight major changes of the field in the directions x (Dx) and y (Dy) (Phillips 2000). Computation of the first vertical derivative (Dz) in an aeromagnetic survey is equivalent to observing the vertical gradient directly with a magnetic gradiometer. It has the same advantages (Fig. 5-B), enhancing shallow sources, suppressing deeper ones, and giving a better resolution of closely spaced sources (Reeves 2005).

The analytic signal represents a technique used to analyze signals in electronics, where a larger amount of information is obtained from a real function through its transformation into a complex function. The quadrature information (imaginary part of the signal) was obtained through the Hilbert transformation of the real part. This concept was presented by Nabighian (1972) when studying the potential fields, in the magnetic case, aiming to find a semi-automated process for the interpretation of the generated sources from a magnetic field. It is based on the horizontal derivative (real part) and vertical derivative (imaginary part) of the magnetic field. This transformation turns the position indications independent from the magnetic latitude where they are located, and the presence of remnant magnetization in the sources involved (Roest et al. 1992), since this indication is more dependent on the horizontal magnetic gradient (Blakely

1996). The analytical signal is used for determining geometric parameters, such as tracing area limits of the sources (either geologic or structural), and it can even supply an estimate of the depths of these sources. This technique was improved since its conception by Nabighian (1974) and others (Rao et al. 1981; Thompson 1982; Murthy 1985; Blakely and Simpson 1986; Blakely 1996). The analytic signal (Fig. 5-C) is a symmetric function, whose peaks are centered on the edges of the anomalous body or the corresponding geologic feature, allowing its mapping (Nabighian 1972, 1984; Roest et al. 1992; Hsu et al. 1996).

The tilt derivative (Fig. 5-D) defines the spatial behavior of the analytic signal vector in the vertical plane that contains the resulting horizontal component of the considered point. It has shown to be efficient when mapping linear features of the magnetic relief (commonly relatable to the textural/structural features of the underlying geologic material) and, due to its spatial arrangement and relative texture, when delimiting the different magnetic units, it enhances features sometimes little apparent on the analytic signal amplitude.

The pseudo-gravity filter was applied to enhance anomalies associated with deep magnetic sources. The data can be modeled using conventional gravimetric modeling tools (Pratt and Shi 2004). The pseudo-gravity map of the southwest of Rondônia exhibits a separation of large tectonic domains that indicate environments of different depths (Fig. 6-A).

4.2. Gamma-ray spectrometry

The concentration values obtained in the gamma spectrometry are derived from a direct relation of the intensity of the captured radiation, and then transformed into equivalent concentrations through mathematical models. The maps showing the gamma spectrometric data were created by interpolation, using the minimum curvature method (Briggs 1974), due to favoring the radiometric anomalies along the flight lines direction (IAEA 2003). The three radioelement channels (Potassium in %, equivalent thorium in ppm and equivalent uranium in ppm) are the base of the subsequent processing (Fig. 7). The final products for analysis are ternary images in RGB (KThU) and CMY (KThU) false-colors (Fig. 8).

The potassium, thorium and uranium concentration maps indicate a lateral variation of concentration of these elements obtained through processing that considers the intensity of the radiation received in a frequency interval characteristic of each radioelement. The received radiation depends on variables such as the concentration of the radioelement in the source, the distance of the detector (flight height), and the humidity level of the source (IEAE 2003). The concentration of these elements in the crust varies according to the rocks nature.

Ternary maps of RGB (KThU) (Fig. 8-D) and CMY (KThU) pseudo-color showed to be an efficient way to represent the lateral variation of the three elements. In these products, the concentration of each radioelement is represented by the variation of color intensity. When combined, they create secondary colors indicating a high concentration of two or more radioelements. Within the context of this study, the K, Th and U values are represented with red, green and blue respectively in the RGB map; and cyan, magenta and yellow respectively in the CMY map.

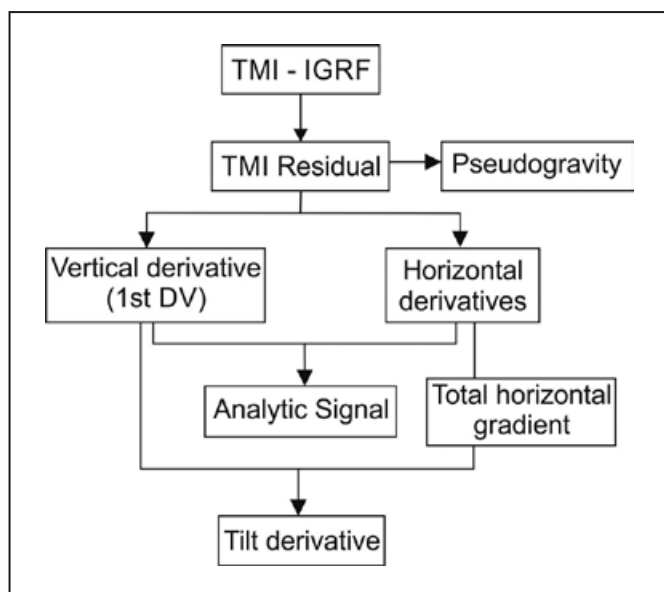


FIGURE 4: Flowchart showing the sequence of airborne magnetometry data processing. TMI - total magnetic intensity; Horizontal derivative - first horizontal derivative in x and y of the TMI; 1VD - first vertical derivative of the TMI; ASA - analytic signal amplitude.

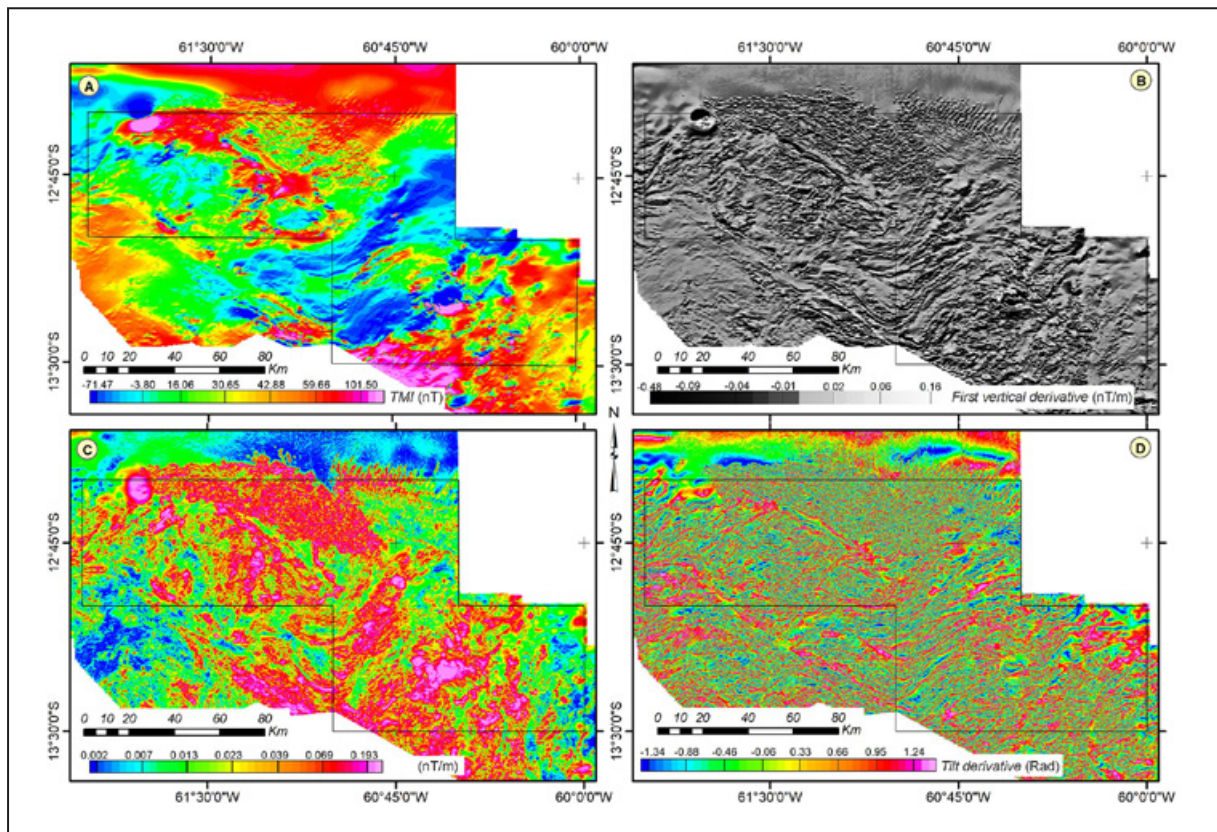


FIGURE 5: (A) Total magnetic intensity – TMI - with shaded magnetic relief and also illumination inclination and declination at 45°; (B) First vertical derivative – 1st VD of the TMI; (C) analytic signal amplitude of the TMI; (D) Analytic signal tilt derivative of the total magnetic intensity.

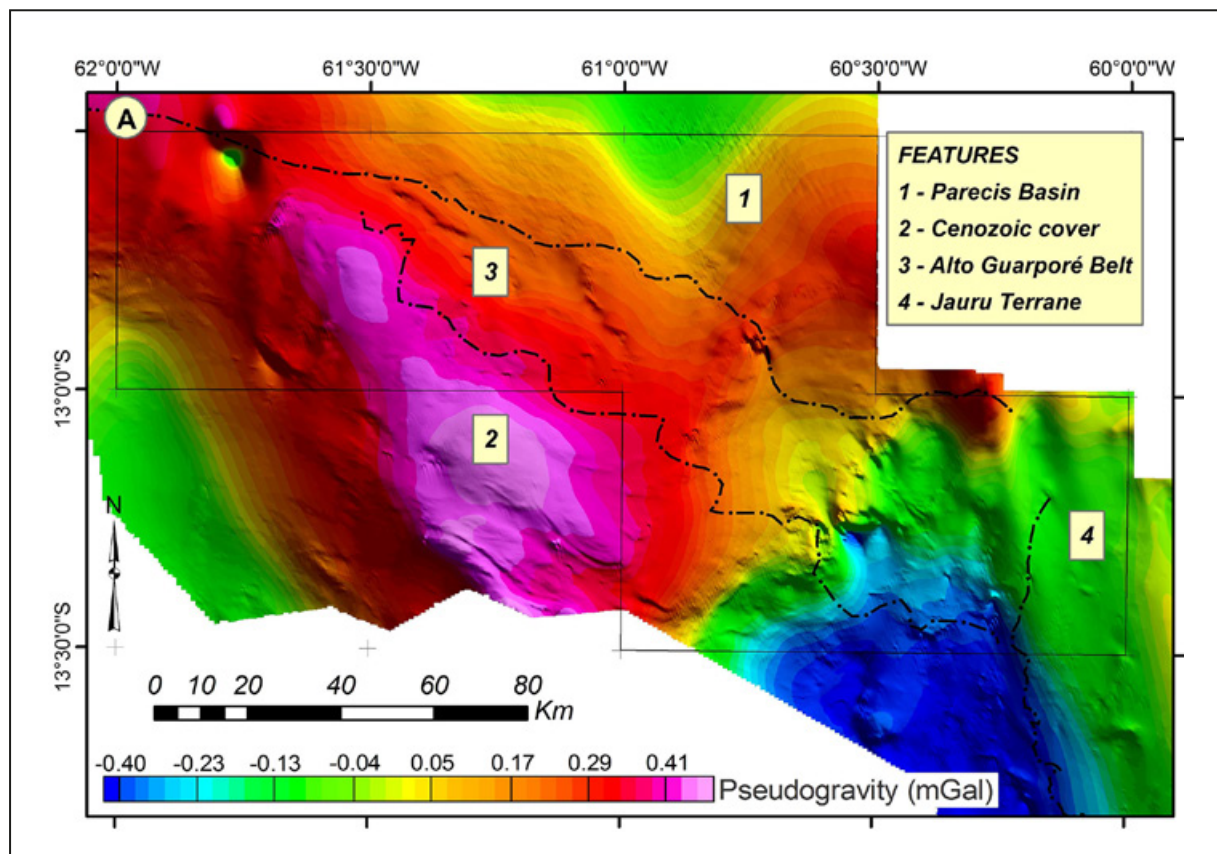


FIGURE 6: Pseudo-gravity map derived from the TMI data.

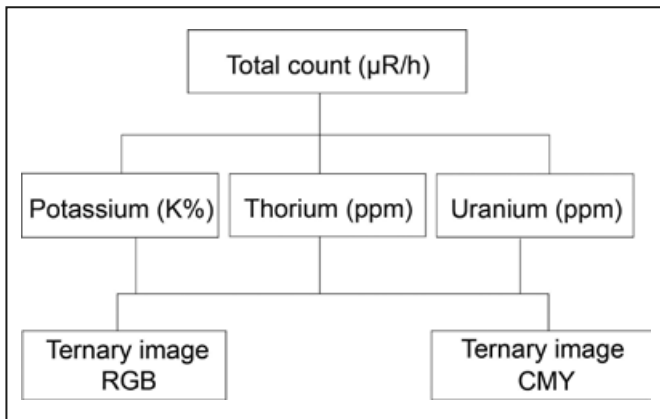


FIGURE 7: Gamma-ray spectrometry data processing flowchart. RGB (KThU) – a ternary false-color image where the concentration of each radioelement is expressed in proportion to the intensity of the primary color. CMY (KThU) - ternary false-color image where the concentration of each radioelement expressed in proportion to the intensity of Cyan, Magenta and Yellow.

5. Interpreted Structural Framework

To analyze the structural framework, images of the vertical derivative and tilt derivative were used. The result of the interpretation of the linear features represents the deformation that affected the region. Based on these observations, three structural domains were defined (D1, D2, D3) in the Alto Guaporé Belt (Fig. 9).

The structures related to the D1 domain are predominant in the study area. However, Cenozoic sediments of the

Guaporé Basin, limiting the use of field structural data, cover a considerable part of these magnetic structures. The D1 structures presents a sinuous geometry with a preferential direction N50W. In the center part of the area, these lineaments flex to NE, in an "S" shape, returning to N50W in the east. This zone was delimited in the analytic signal map by an increase in the magnetic amplitude and in the density of magnetic lineaments. The morphology of these lineaments suggests sinistral movement, where the crustal segment located in the east shifted to NE in relation to the crustal segment in the west of the area. In the east, the interpretation exhibits a zone approximately 32 km wide by 36 km long with high magnetic amplitude and large density of magnetic lineaments in N50W direction. This zone is limited in the east by a strong magnetic gradient characterized by anastomosed structures in a NNW trend, which truncate the structures of the domain D1, delimiting the D2 pattern.

According to Rizzotto (2010) and Rizzotto et al. (2013), the structuration of the Alto Guaporé Belt is characterized by large ductile shear zones and syntectonic crenulation that aligns with previous structures. By analogy, the D1 domain is probably related to these structures, and was formed between 1.459 and 1.329 Ma, according to geochronological data (Rizzotto et al. 2013). The D2 domain is associated with anastomosed lineaments with a NNW trend verified in the southeastern region of the area. These lineaments truncate the D1 linear structures and characterize the strong magnetic gradient that delimits the magnetic crustal segment in the west and a weak magnetic crustal segment in the east. This discontinuity follows the same structural trend of the Rio Vermelho lineament (Pindaituba Intrusive Suite) in the Jauru Terrane.

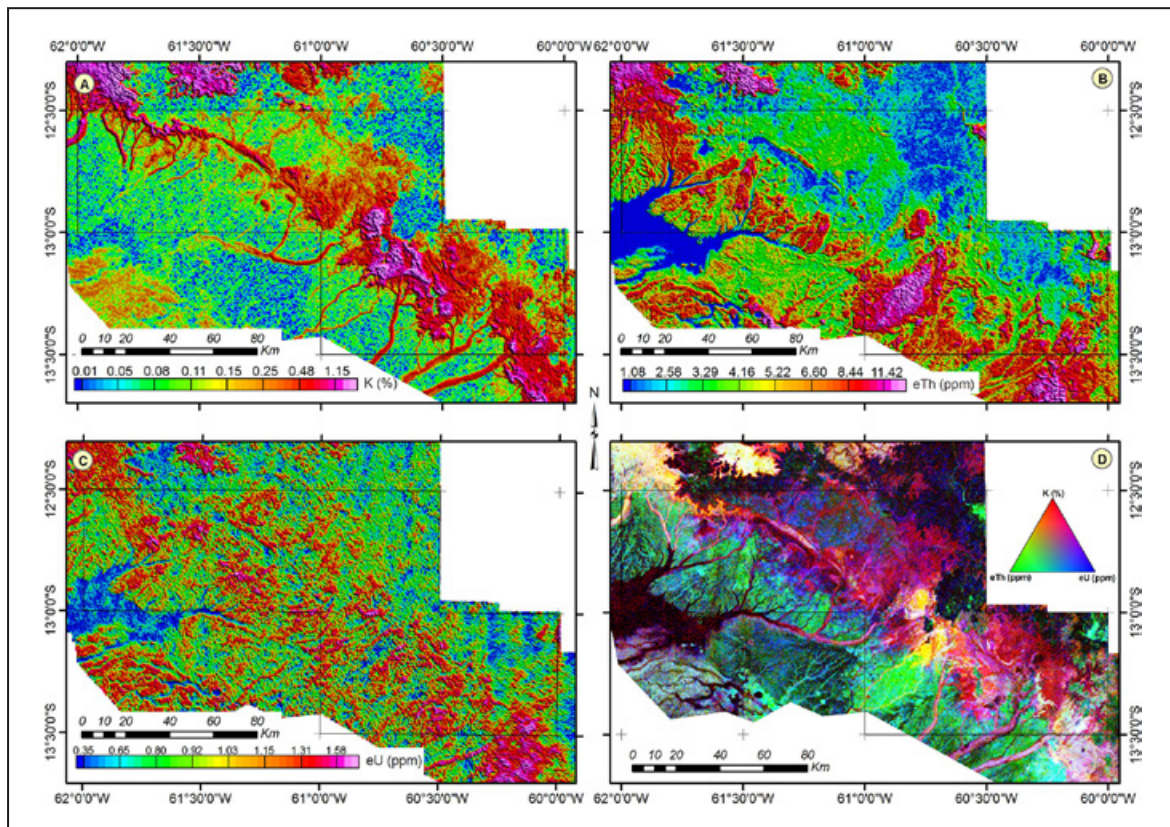


FIGURE 8: Airborne gamma spectrometric maps, where: (A) radiometric map of potassium distribution - K; (B) radiometric map of thorium distribution - eTh; (C) radiometric map of uranium distribution - eU; (D) radiometric map of the ternary composition – RGB.

The D3 domain is characterized by large straight magnetic lineaments with N35E, EW, N50W, and N20W directions that cut through the whole research area. These lineaments are possibly related to brittle structures that reproduce the crustal anisotropy generated during the D1 and D2 events. Greater density of these magnetic lineaments is observed on the northern part of the area, which corresponds to the southern border of the Colorado Graben, Parecis Basin. These structures were possibly activated during the Parecis Basin opening in the Paleozoic.

The analytic signal (AS) of the upward continuation of 10 km and the pseudo-gravity map allowed the identification of features and magnetic lineaments related to the deep structuration of the crust in the region of Alto Guaporé. There are lineaments observed in two preferential directions: N35E and N50W. The discontinuities defined by these lineaments coincide with the truncation and interference of shallow lineament structure zones, indicating that the discontinuities can be related to the accretion of terranes, evidenced by the different magnetic signatures, defining the limits between the Alto Guaporé Belt and Jauru Terranes, previously defined by Rizzotto et al. 2013 (Fig. 10).

6. Interpreted Lithological Framework

6.1. Magnetic Domains

The identification of magnetic domains is essential for the data qualitative interpretation and involves the delimitation of areas with different magnetic anomaly patterns that must represent different geologic units (Reeves 2005). Due to the geologic complexity and the size of the area, a reclassification of the AS defined five uniform classes, based on the resampling of values in nT/m, shown in Table 2. The qualitative interpretation shows five classes of magnetic domains (Fig. 11). The magnetic domains were discriminated according to the texture and intensity of the magnetic response.

Five main domains were mapped (H-1, H-2, H-3, H-4 and H-5) based on the analytic signal amplitude with high gradient (values > 0.225 nT/m) (Fig. 11). The H-1 domain is characterized by a local anomaly in the southeastern portion of the area. It has a round format with a diameter of approximately 7 km and represents the I-type granites of the Igarapé Enganado Intrusive Suite and ultramafic rocks of the

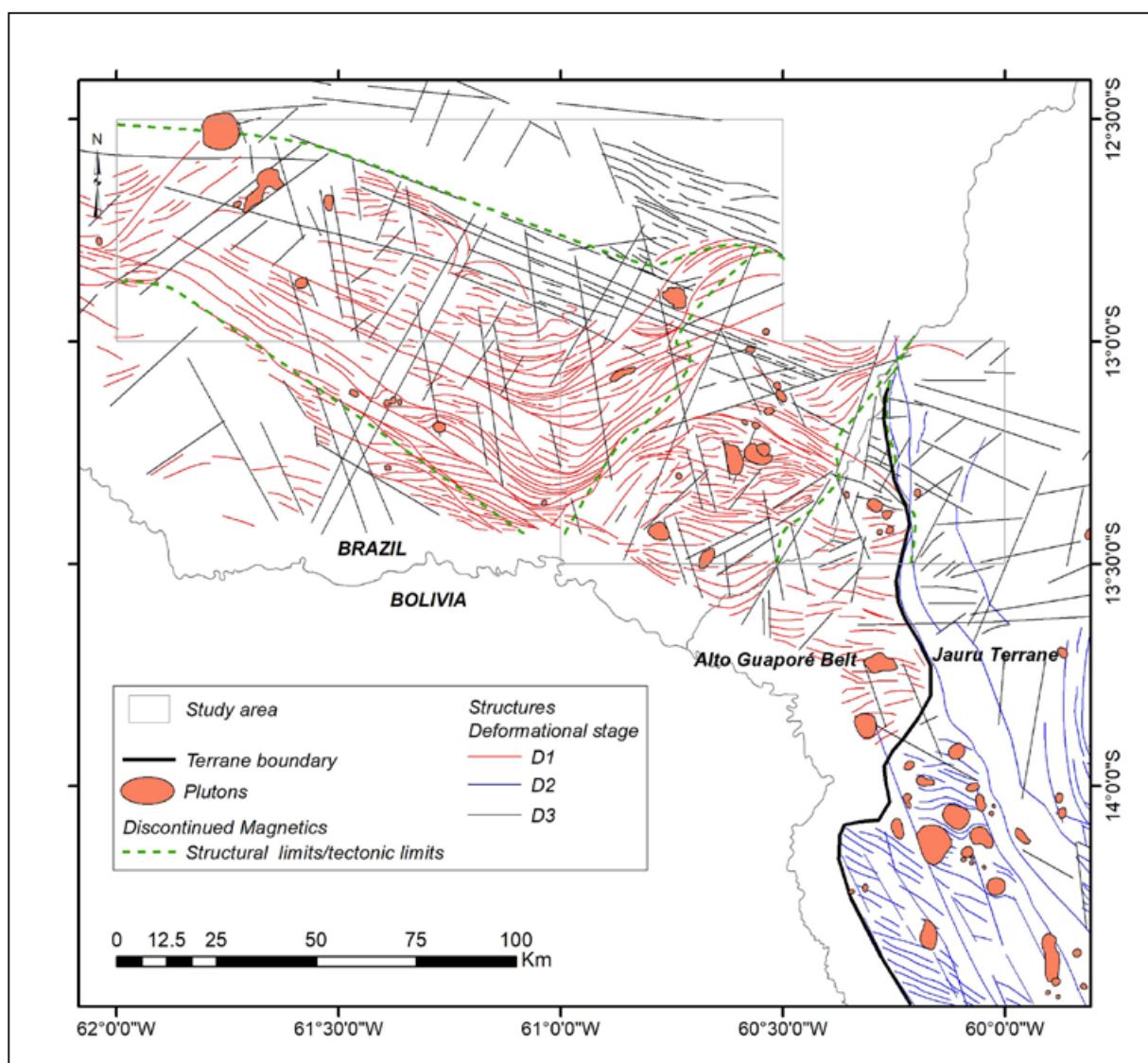


FIGURE 9: Magnetic structural map interpreted from the horizontal and vertical derivatives and the tilt derivative, emphasizing the distinction of the magnetic patterns.

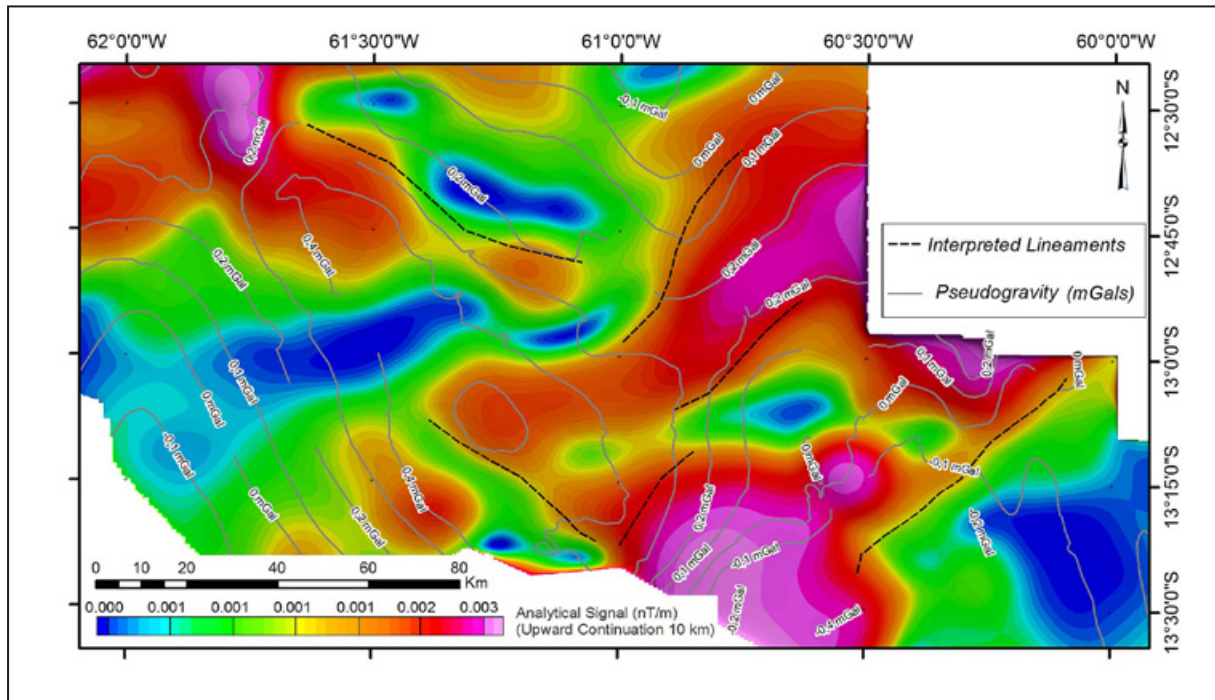







FIGURE 10: Analytic Signal map from 10 km the upward continuation TMI. The contour lines were extracted from the pseudo-gravity map.

TABLE 2 - Analytic Signal Amplitude Classes. The reclassification allowed the differentiation of large magnetic domains, mafic/ultramafic bodies, I-type granites.

Analytical Signal	Range (nT/m)	Rocks	Symbol
High(H)	> 0.224	Trincheira Complex, mafic plutons, banded iron formation and I-type granites	
Medium to high (MH)	0.082 – 0.224	Trincheira mafic-ultramafic complex, mafic granulites and Anari basalt	
Medium (M)	0.021 – 0.081	Covered granitic plutons, Colorado Complex	
Medium to low (ML)	0.006 – 0.020	Sedimentary covers	
Low(L)	< 0.006	Rio Galera Complex and Pindaituba Suite	

Trincheira Complex. To the north of this anomaly, there is the H-2 domain, which shows elongated features with a NW/SE direction and extends for approximately 25 km, representing mafic bodies and metapelites of the Trincheira Complex. A round anomaly represents the H-3 domain with a diameter of 4 km located in the central region of the area, highlighting the body of the Alto Escondido Intrusive Suite. The H-4 domain presents an elongated anomaly with a NE/SW direction with an extension of 15 km along the major axis, with a predominance of ASA values higher than 0.225 nT/m. In a geological sense, this signature represents the mafic-ultramafic Serra Céu Azul Suite body, defined as olivine-gabbro and metagabbro with potential for Cr, Ni and Cu (Romanini 1997). The H-5 domain, in the northwest portion of the area, has a round format with

a diameter of approximately 10 km, and a predominance of medium to high magnetic intensity values.

The MH-1 domain, with a predominance of medium to high classes (0.082 - 0.224 nT/m), is defined by anomalies of small amplitudes of analytic signal in the middle of a rough texture, some of them with an elongated format with an inflection of the magnetic structure from N50W to N35E in the center of the domain, suggesting a large crustal discontinuity defined by faults that show a predominant sinistral component. In the south of this domain, elongated anomalies with N50W direction extend over 40 km and are associated with smaller anomalies, extending 7 km. The correlation with the geological units is complex due to the Cenozoic sedimentary covers of the Guaporé Basin. The outcropping basement is correlated to

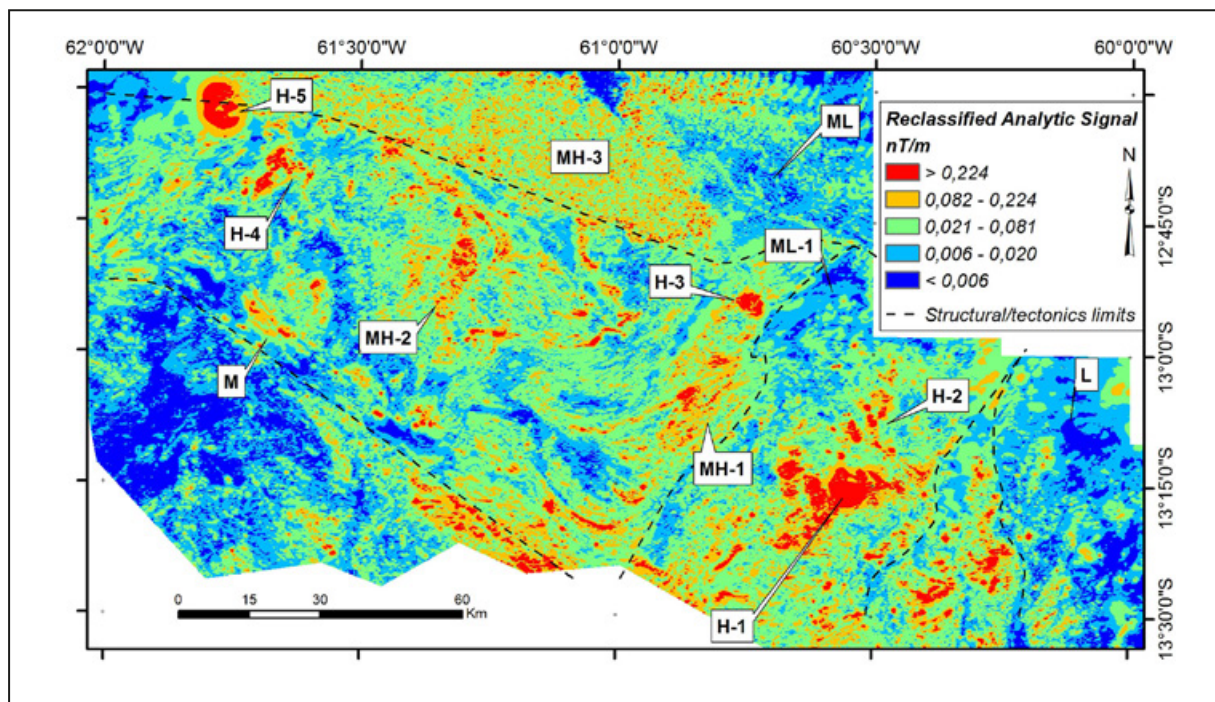


FIGURE 11: Magnetic map from reclassified analytic signal amplitude. The differences between the magnetic ranges based in the reclassification highlight the textures of the magnetic domains. The labels indicate magnetic domains described in the text.

the Mafic-Ultramafic Trincheira Complex, where the magnetic data show the continuity of this unit below the basin sediments. The MH-2 domain has an extension of approximately 25 km along its major axis, aligned NNE, and has a rough magnetic texture with the highest magnetic classes located on the north side of the domain, correlated to mafic granulites of the Trincheira unit. The MH-3 domain presents a characteristic texture with a predominance of anomalies of small wavelength and a magnetic intensity varying from medium to medium-high, with some anomalous peaks above 0.225 nT/m. This domain extends for 100 km along its major axis and correlates to the basalts of the Anari Formation. The high frequency of the anomalies and disappearance in the upward continued data suggests that the magnetic sources of the domain are close to the surface.

The M domains represent anomalies of average magnetic intensity constituting the periphery of the greatest amplitude domains. These domains show curved features imposed by deformation following a regional trend. In geologic terms, this domain can be correlated to some granitic bodies and the basement, represented by the Colorado Complex.

The ML and L domains are characterized as magnetic lows, with large dimensions, that occur all over the research area, and represent the geological framework with a less rough magnetic relief. On the north side, the medium to low magnetic (ML) is generally associated to the Parecis Basin. In the southeastern portion of the area, the low values of magnetic susceptibility (L domain) highlighted rocks of the Pindaituba Intrusive Suite and Rio Galera Complex in the Jauru Terrane.

6.2. Gamma-ray spectrometry domains

Gamma-ray spectrometry is an important source of information for soil, regolith and geomorphologic studies. It

perfectly reveals the primary lithologic information and the geochemistry of the first 30 cm of the ground (Wilford et al. 1997; Minty 1997).

Elaboration of the gamma spectrometric domain map consisted of the analysis and discrimination of regions, where the radiometric response is similar in terms of textures and radioelement concentration. As a final product, thirteen distinct domains were differentiated and classified in high, medium and low value according to the equivalent concentrations of potassium, thorium and uranium (Fig. 12). In order to correlate, the colors used to represent the domains were the same used on the RGB ternary map (K, eTh, eU). This evaluation made possible the correlation of the lithologic units with the map of gamma-ray spectrometry domains (Fig. 12).

The domains with a high concentration of the three radioelements highlight the external zones of the plutons of Cerejeiras and Alto Escondido, and they are also associated with schists and paragneisses of the Colorado Complex combined with granitic bodies concordant with the metamorphic foliation. In the core of the granitic plutons of Cerejeiras and Alto Escondido there are zones enriched in K and eTh, and relatively depleted of eU. The units enriched in K and eTh, and depleted of the other radioelements can similarly be correlated with the lithotypes of the Igarapé Enganado Intrusive Suite (Fig. 12).

The radiometric units enriched in K and eTh and moderately depleted in eU represent the units of the Parecis Basin, in the northeastern side of the area, as well as the broad drainages that transport large quantities of sediments in the Rio Escondido valley.

The rocks of the Colorado Complex and the Igarapé Hermes Intrusive Suite, in the southeastern portion of the area, are represented by radiometric units enriched in K and eU and depleted of eTh, corresponding to magenta shades on the RGB ternary map.

The units enriched in eTh, although varying in relation to the other elements, are attributed to the Phanerozoic covers of the Guaporé Basin, and these domains together cover the majority of the study area. Units enriched in eU and depleted in the other elements, occur in regions of the Guaporé Basin edge and are also observed in some rocks of the Trincheira Complex. In this perspective, the mafic and ultramafic rocks of the Trincheira Complex, sedimentary rocks of the Parecis Basin and flooded areas on the Guaporé plain reflect radiometric units depleted in the three elements.

The basalts of the Anari Formation and the regolithic material, which resulted from the weathering on these rocks, present a reduction in the percentage of K and medium concentrations of eTh and eU. The Fazenda Casa Branca Formation sedimentary rocks also show intermediate responses of eTh and eU, though with textural signature different from the Anari Formation.

7. Isotopic and geochronological data of igneous rocks of the Alto Guaporé Belt and regional magmatism.

The association of mafic and felsic rocks of varied nature and ages represents an important component of the Guaporé Belt. The emplacement and metamorphism ages of the mafic and felsic rocks, combined with the isotopic composition of Nd, are essential to understand the belt tectonic evolution. Despite the "poor" precision of the Sm-Nd analysis of mafic rocks, its model crystallization ages and initial isotopic ratios supply important information about the geological history of this Mesoproterozoic terrane (Fig. 13).

U-Pb data on dioritic gneiss of the Colorado Complex, which have three populations of zircons grains, indicated three different ages: 1344 ± 7 Ma (metamorphic), 1469 ± 5 Ma (magmatic) and 1539 ± 9 Ma (inherited). The youngest is interpreted as the metamorphism age of the collisional phase (Rizzotto et al. 2013).

Sm-Nd and Sr isotopes data presented by Rizzotto et al. (2013) of the Mafic-ultramafic Trincheira Complex provided values of initial ratio 87Sr/86Sr (Sri), 143Nd/144Nd (Ndi), εSr(T) and εNd(T), calculated based on the igneous crystallization age of 1460 Ma. The Sri values for mafic rocks vary from 0.7002 to 0.7033, the Ndi varies from 0.5120 to 0.5133 and positive values of εNd(T) (+2.6 to +8.8) are seen, indicating that the basaltic predecessors were derived from a depleted mantle source. The rocks of this unit can also be correlated to the Santa Isabel Formation (southwest of Mato Grosso State) which includes amphibolites, meta-ultrabasic rocks, metabasalts, metagabbros and serpentinites (Matos et al. 2004).

Rizzotto et al. (2013) reported a 1347 ± 8 Ma igneous crystallization age from the mafic-ultramafic rocks of the Igarapé Hermes. In this work, the authors further show a Sm-Nd analysis on metagabbro, using crystallization age lower than 1100 Ma, finding a TDM age of 1.17 Ga and εNd of +5.2. Within this context, the Colorado mafic Intrusive Suite has crystallization ages of 1344 ± 8 and 1354 ± 11 Ma and εNd between +2.7 and +5.4. The analysis of these data suggests a new juvenile magmatism event at the late Mesoproterozoic.

Rocks from the Igarapé Enganado Suite, from Rizzotto (2010) for zircons from granodiorite using the U-Pb - SHRIMP method, supplied intercept age of 1340 ± 5 Ma, interpreted as

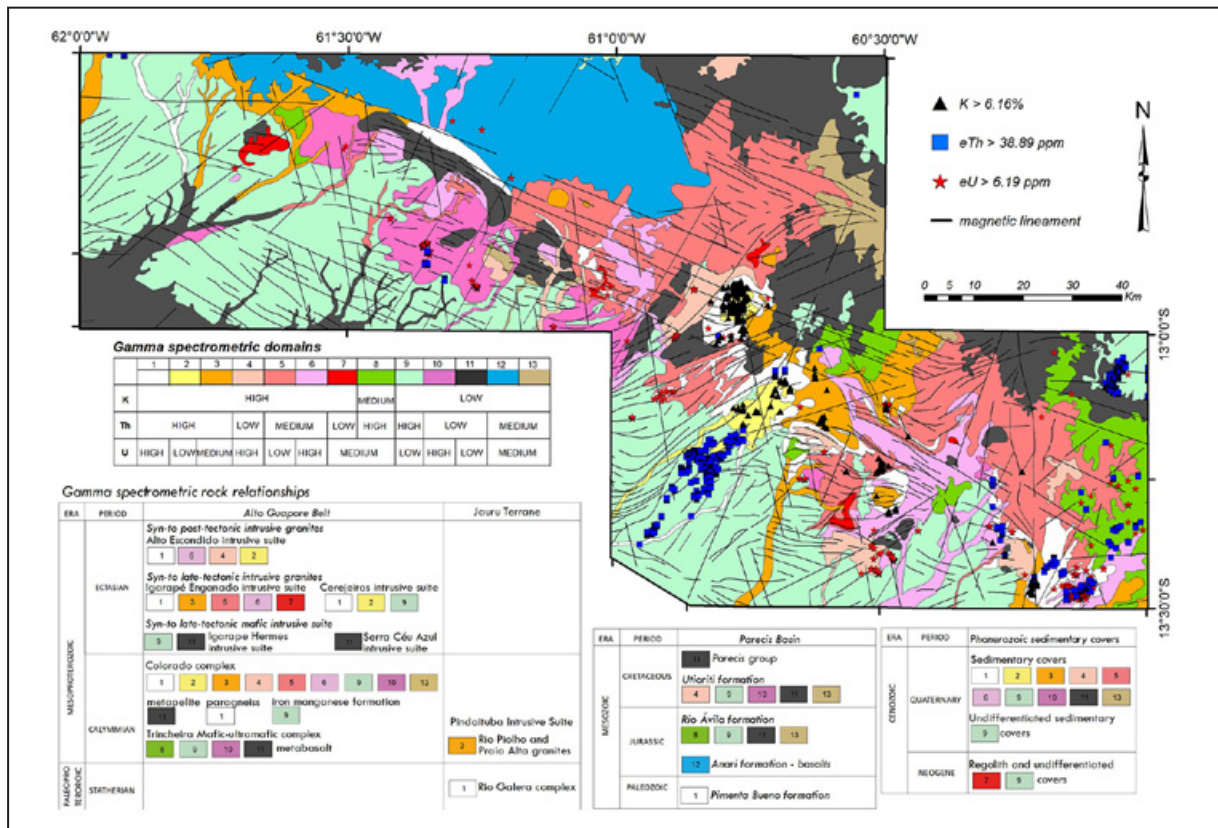


FIGURE 12: Gamma-ray spectrometry domains map in the research area. Based on the interpretation of the different maps of radioelements with previous geologic data. The rocks units with their respective gamma-ray signature are indicated.

rock crystallization age. Analysis of Sm-Nd isotopes gave TDM ages from 1.58 to 1.51 Ga and ϵNd of +2.33, interpreted as the time of extraction of mantle material. The suite was dated using the U-Pb isotopic system via SHRIMP by Bettencourt et al. (2010), who used samples of monzogranite and syenogranite, with concordia ages of 1340 ± 5 Ma. The rocks in the eastern portion of Bolivia are correlated to this unit (Litherland et al. 1986; Boger et al. 2005), such as the San Rafael Granite of U-Pb age 1334 ± 12 Ma and the granites of the Alto Candeias Intrusive Suite on the western side of Rondônia.

Rizzotto (2010) determined geochronological data in the Alto Escondido Suite using the U-Pb method on zircon. The U-Pb data supplied an intercept age of 1340 ± 3 Ma, interpreted as the crystallization age. The Sm-Nd method gave values of ϵNd ($T=1.3$ Ga) of +2.35 and TDM model ages of 1.51 Ga, which indicate a primitive mantle source for these rocks. The authors also determined U-Pb data for a syenogranite with an intercept age of 1337 ± 4 Ma. The values for the Sm-Nd method were ϵNd ($T=1.3$ Ga) of +1.55 and TDM model age of 1.58 Ga, also indicating a juvenile source with a short crustal residence protolith. Rizzotto (2010) used muscovite crystals from the aplitic leucogranite, product of metamorphism, yielded ^{40}Ar - ^{39}Ar , ages of 1312 ± 3 Ma, interpreted as the age of the regional metamorphic cooling.

Rizzotto (2010) analyzed zircon of a sample of the Praia Alta Granite using the U-Pb-LA-MC-ICP-MS method finding ages of 1432 ± 13 Ma, interpreted as ages of rock crystallization. Ages of Rizzotto et al. (2013) in zircon of biotite syenogranite using the U-Pb-LA-MC-ICP-MS method, included imaging via cathodoluminescence highlighting crystals with prismatic habits and 100 to 200 mm in size, and metamorphic rims pattern. Nevertheless, the contents of U and Th supplied median values, creating Th/U between 0.13 and 0.59, which suggest grains of igneous origin. SHRIMP analysis in zircon of this rock gave average ages of the $^{207}\text{Pb}/^{206}\text{Pb}$ ratios of 1436 ± 7 Ma, interpreted as crystallization age. The second analyzed sample, syenogranite (the same rock dated by Rizzotto 2010), showed large well-faceted zircon crystals. The U-Pb LA-MC-ICP-MS analysis of zircon yielded Th/U ratios varying between 0.24 and 0.42, indicating magmatic origin, and the concordia age of 1426 ± 5 Ma. This age was interpreted as the igneous rock crystallization age.

Ruiz (2005) reported U-Pb geochronological data from biotite monzogranite of the Pindaituba Suite (sample from the Morro Sem Boné Sheet) on yellowish, prismatic, medium size zircon crystals. Ages of upper intercept of 1423 ± 11 Ma were obtained and interpreted as the rock igneous crystallization age. The isotopic Sm-Nd data of this rock supplied by Ruiz (2005) present TDM model ages of 2.0 Ga, which indicates mantle differentiation at the beginning of the Orosirian. A positive value was obtained for $\epsilon\text{Nd}(t)$ of 0.91, which indicates a predominant mantle source, although with crustal contamination for the protolith of this rock.

8. Discussion and conclusions

The airborne geophysical data show that the southeastern part of the Rondônia State and northwestern part of Mato Grosso carries a complex tectonic history with distinct events of superimposed deformation. The Phanerozoic sedimentary beds, and layers (Parecis and Guaporé basins) cover a

significant part of the region, making the mapping of important geological features of the basement difficult. Therefore, it is essential to integrate airborne geophysical data as well as data collected in the field for the advancement in the geological understanding of the region.

The magnetic data analysis allowed the separation of crustal segments with distinct magnetic signatures, assisting in the tectonic understanding of the region. The extraction of the structural features allowed to characterize the structural framework of the region. The signatures of magnetic structures of deep source show two main trends, N50W and N35E. These lineaments probably represent large crustal discontinuities related to the accretion of terranes with distinct magnetic signatures and are associated with the limits between the Alto Guaporé Belt and the Paraguá and Jauru terranes. The map of pseudo-gravity of the area emphasizes the presence of these deep discontinuities. The shallowest magnetic lineaments, extracted from the analytic signal, were assigned to different deformation periods by analyzing cross-cutting relations. The upward continued data enabled the identification of three distinct structural domains in the region. The oldest lineaments related to the D1 pattern are probably associated with the Rondonian-San Ignacio orogeny between the Paraguá Terrane and the Amazonian proto-craton, described by Loewy et al. (2004), Boger et al. (2005) and Rizzotto and Hartmann (2012). The lineaments related to the D2 domain are less apparent and follow the same structural trend of the Rio Vermelho lineament (Pindaituba Intrusive Suite) in the Jauru Terrane, northwest of the Mato Grosso State, associated to the Sunsás orogeny. The D3 domain is characterized by prominent straight magnetic lineaments related to brittle structures, which used the crustal anisotropy generated during the D1 and D2 events. These structures were possibly activated during the opening of the Parecis Basin in the early Paleozoic.

The integration of the radiometric data permitted creating the gamma-ray spectrometry domains map, which enabled the discrimination of the Phanerozoic sedimentary basins and of the rocks that make up the Proterozoic basement. From this analysis, it is possible to observe the influence of the sedimentary cover of the Guaporé Basin in the southwestern portion of the study area and rocks of the Parecis Basin in the northern and northeastern portions. Thus, the basement rocks are limited to a narrow northwest/southeast oriented zone, partially concordant with its internal structure. Later on, it was verified that these radiometric signatures correlated with the geologic units mapped, or with hydrographic features present in the region.

The Sm-Nd isotopic data of the mafic and felsic rocks of the region are similar and suggest a unique tectonic domain, except for the mafic-ultramafic Igarapé Hermes rocks with TDM values of 1.17 Ga and ϵNd of +5.2. Strongly positive values of ϵNd (T) (+2 to +9) for the rocks of the Trincheira Complex are compatible with the absence of crustal contamination of the original magma, a fact coherent with the oceanic environment in which the mafic rocks probably originated. The intermediate to acid rocks of calc-alkaline composition, Igarapé Enganado and Rio Escondido suites, showed sources with a longer period of crustal residence (TDM 1.51 to 1.63 Ga) and values of ϵNd of +1.5 to +2.33 suggesting a subordinated contribution of crustal material. On the other hand, the Praia Alta Granite,

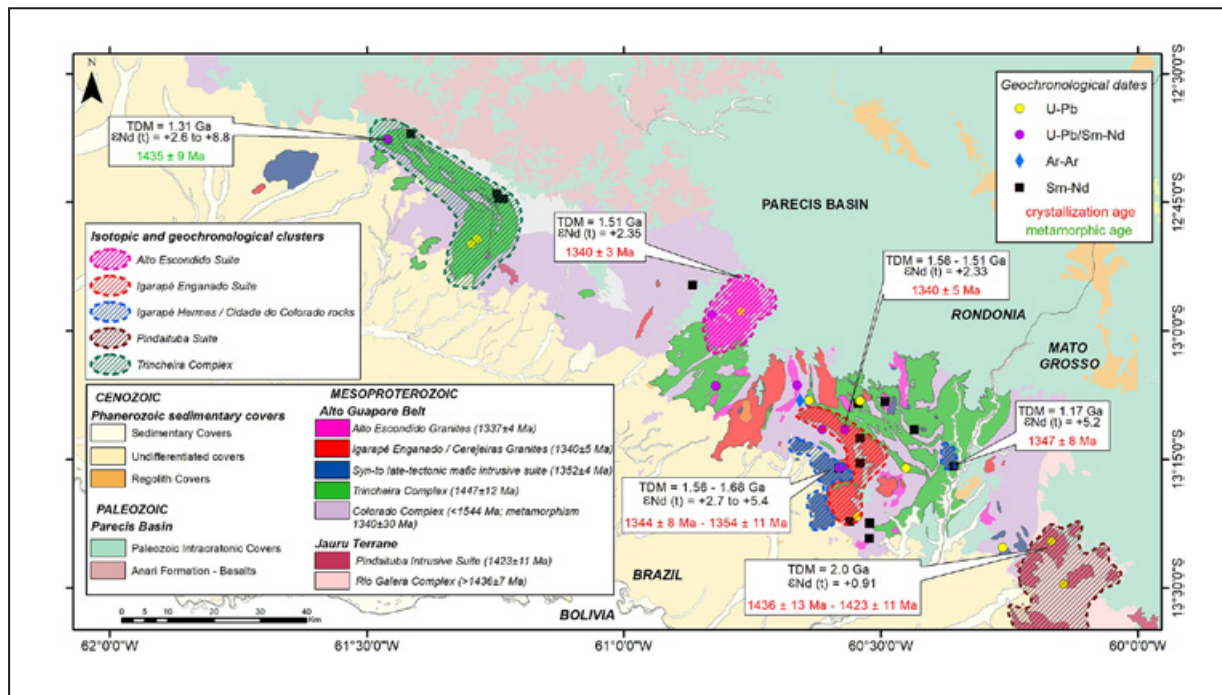


FIGURE 13: Gamma-ray spectrometry domains map in the research area. Based on the interpretation of the different maps of radioelement Geochronological data source (compiled from Ruiz 2005; Scandolaro 2006; Rizzotto 2010; Rizzotto et al. 2013).

with a crystallization age of 1423 ± 11 Ma shows a TDM model age of 2.0 Ga and $\epsilon Nd(t)$ pattern of 0.91, which indicates a mantle source, although with an important crustal component for the protolith.

The geodynamic history and geologic architecture are important parameters for the definition of mineral systems and the development of mineral exploration targets models at regional and local scales. The application of this kind of procedure is the first step for the understanding of the mineralizing processes. Thus, the results of the study can be summarized as follows:

1. The limit of the Alto Guaporé Belt with the Jauru Terrane is well delimited by both gravimetry and magnetometry, suggesting a distinct geotectonic evolution;
2. The Alto Guaporé Belt structures indicate a variation from NW to NE, pointing a more complex kinematic;
3. The integration of airborne geophysical data shows different structural domains.

Authorship credits

Author	A	B	C	D	E	F
CESO						
AMS						
JES						

A - Study design/Conceptualization
 B - Investigation/Data acquisition
 C - Data Interpretation/Validation
 D - Writing
 E - Review/Editing
 F - Supervision/Project administration

Acknowledgements

We thank the Geological Survey of Brazil (CPRM) for the access to the airborne geophysical, geological and geochronological data, especially the geologists Elias Martins and Guilherme Ferreira for the support during the fieldwork.

Special thanks also belong to the CPRM for and financial support (process no. ATA1135/memo101/SEGER/2014), and the University of Brasília for the technical support and permission of laboratory use as well as Bianca Takenaka for help with geochronological data. A. M. Silva thanks the National Council for Scientific and Technological Development (CNPq) for her research grant.

References

- Bahia R.B.C., Martins-Neto M.A., Barbosa M.S.C., Pedreira A.J. 2007. Análise da evolução tectonossedimentar da Bacia dos Parecis através de métodos potenciais. *Revista Brasileira de Geologia*, 37(4), 639-649. Available on line at: <https://ppegeio.igc.usp.br/index.php/rbg/article/view/9239> / (accessed on 14 April 2022)
- Bahia R.B.C., Pedreira A.J. 1998. Estratigrafia, sedimentação e tectônica da cobertura fanerozóica do estado de RO. In: Congresso Brasileiro de Geologia, Belo Horizonte, 40, 102. Available on line at: http://sbge.sitepessoal.com/anais_digitalizados/1998-BELO%20HORIZONTE/CBG1998.pdf / (accessed on 14 April 2022)
- Baranov V. 1957. A new method for interpretation of aeromagnetic maps: pseudo-gravimetric anomalies. *Geophysics*, 22(2), 359-382. <https://doi.org/10.1190/1.1438369>
- Bettencourt J.S., Leite W.B., Ruiz A.S., Matos R., Payolla B.L., Tosdal R.M. 2010. The Rondonian-San Ignacio Province in the SW Amazonian Craton: an overview. *Journal of South American Earth Sciences*, 29, 28-46. <https://doi.org/10.1016/j.jsames.2009.08.006>
- Blakely R.J. 1996. Potential theory in gravity and magnetic applications. Cambridge, UK, Cambridge University Press, 441p.
- Blakely R.J., Simpson R.W. 1986. Approximating edges of source bodies from magnetic or gravity anomalies. *Geophysics*, 51(7), 1494-1498. <https://doi.org/10.1190/1.1442197>
- Boger S.D., Raetz M., Giles D., Etchart E., Fanning M.C. 2005. U-Pb age data from the Sunsas region of Eastern Bolivia, evidence for the allochthonous origin of the Paraguá Block. *Precambrian Research*, 139(3-4), 121-146. <https://doi.org/10.1016/j.precamres.2005.05.010>
- Briggs I.C. 1974. Machine contouring using minimum curvature. *Geophysics*, 39(1), 39-48. <https://doi.org/10.1190/1.1440410>
- Cooper G.R.J., Cowan D.R. 2006. Enhancing potential field data using filters based on the local phase. *Computers & Geosciences*, 32(10), 1585-1591. <https://doi.org/10.1016/j.cageo.2006.02.016>

- Cordani U.G., Brito Neves B.B. 1982. The geologic evolution of South América during the Archean and Early Proterozoic. *Revista Brasileira de Geologia*, 12(1-3), 78-88. Available on line at: <https://www.ppegeo.igc.usp.br/index.php/rbg/article/view/12193> / (accessed on 14 April 2022)
- Cordani U.G., Tassinari C.C.G., Teixeira W., Basei M.A.S., Kawashita K. 1979. Evolução tectônica da Amazônia com base em dados geocronológicos. In: Congresso Geológico Chileno, 2, Arica, Chile, 137-148.
- CPRM - Serviço Geológico do Brasil. 2006. Projeto aerogeofísico sudeste de Rondônia: relatório final de levantamento e processamento dos dados magnetométricos e gamaespectrométricos. Rio de Janeiro, Prospectores Aerolevantamentos e Sistemas, 27v. Available on line at: <https://rigeo.cprm.gov.br/handle/doc/11283> / (accessed on 14 April 2022)
- Fedi M., Florio G. 2001. Detection of potential fields source boundaries by enhanced horizontal derivative method. *Geophysical prospecting*, 49, 40-58. <https://doi.org/10.1046/j.1365-2478.2001.00235.x>
- Gunn P. J., Mairdment D., Milligan P.R. 1997a. Interpreting aeromagnetic data in areas of limited outcrops. *AGSO Journal of Australian Geology and Geophysics*, 17(2), 175-185. Available on line at: <http://pid.geoscience.gov.au/dataset/ga/81501> / (accessed on 25 April 2022)
- Gunn, P.J., Milligan, P., Mackey, T., Liu, S., Murray, A., Mairdment, D., Haren, R. 1997b. Geophysical mapping using the national airborne and gravity datasets: an example focusing on Broken Hill. *AGSO Journal of Australian Geology and Geophysics*, 17(1), 127-136. Available on line at: <https://ecat.ga.gov.au/geonetwork/srv/eng/catalog.search#/metadata/81484> / (accessed on 25 April 2022)
- Hsu S.K., Sibuet J. C., Shyu C.T. 1996. High-resolution detection of geological boundaries from potential-field anomalies: An enhanced analytic signal technique. *Geophysics*, 61(2), 373-386. <https://doi.org/10.1190/1.1443966>
- IAEA. 2003. Nuclear Fuel Cycle and Materials Section. Guidelines for radioelement mapping using gamma ray spectrometry data. Austria, International Atomic Energy Agency. Available on line at: https://www-pub.iaea.org/mtcd/publications/pdf/te_1363_web.pdf / (accessed on 27 April 2022)
- Jaques A.L., Wellman P., Whitaker A., Wyborn D. 1997. High-resolution geophysics in modern geological mapping. *AGSO Journal of Australian Geology and Geophysics*.17(2), 159-173. Available on line at: <http://pid.geoscience.gov.au/dataset/ga/81500> / (accessed on 27 April 2022)
- Kroonenberg S.B. 1982. A Grenvillian Granulite Belt in the Colombian Andes and its relation to the Guiana Shield. *Geologie en Mijnbouw*, 61, 325-333.
- Litherland M., Annels R.N., Appleton J.D., Berrange J.P., Bloomfield K., Burton C.C.J., Darbyshire D.P.F., Fletcher C.J.N., Hawkins M.P., Klinck B.A., Llanos A., Mitchell W.I., O'Connor E.A., Pitfield P.E.J., Power G., Weeb B.C. 1986. The Geology and Mineral Resources of the Bolivian Precambrian Shield. London, HMSO, 153 p. (Overseas Memoir, Institute of Geological Sciences 9). Available on line at: <https://pubs.bgs.ac.uk/publications.html?pubID=B04055> / (accessed on 27 April 2022)
- Litherland M., Annels R.N., Darbyshire D.P.F., Fletcher C.J.N., Hawkins M.P., Klinck B.A., Mitchell W.I., O'Connor E.A., Pitfield P.E.J., Power G., Webb B.C., 1989. The proterozoic of Eastern Bolivia and its relationship to the Andean mobile belt. *Precambrian Research*, 43, 157-174. [https://doi.org/10.1016/0301-9268\(89\)90054-5](https://doi.org/10.1016/0301-9268(89)90054-5)
- Loewy S.L., Connelly J.N., Dalziel I.W.D. 2004. An orphaned basement block: The Arequipa-Antofalla Basement of the central Andean margin of South America. *Geological Society of America Bulletin*, 116 (1/2), 171-187. <https://doi.org/10.1130/B25226.1>
- Matos J.B., Schorscher J.H.D., Geraldes M.C., Sousa M.Z.A., Ruiz A.S. 2004. Petrografia, geoquímica e geocronologia das rochas do Orógeno Rio Alegre, Mato Grosso: um registro de crosta oceânica mesoproterozóica no SW do Cráton Amazônico. *Geologia USP, Série Científica*, 4, 75-9. <https://doi.org/10.5327/S1519-874x2004000100005>
- Metelka V., Baratouxa L., Naba S., Jessell M.W. 2011. A geophysically constrained litho-structural analysis of the Eburnean greenstone belts and associated granitoid domains, Burkina Faso, West Africa. *Precambrian Research*, 190, 48- 69. <https://doi.org/10.1016/j.precamres.2011.08.002>
- Miller H.G., Singh V. 1994. Potential field tilt a new concept for location of potential field sources. *Journal of Applied Geophysics*, 32, 213-217. [https://doi.org/10.1016/0926-9851\(94\)90022-1](https://doi.org/10.1016/0926-9851(94)90022-1)
- Milligan P.R., Gunn P.J. 1997. Enhancement and presentation of airborne geophysical data. *Journal of Australian Geology and Geophysics*, 17(2), 63-75. Available on line at: https://inis.iaea.org/search/search.aspx?orig_q=RN:28049084 / (accessed on 27 April 2022)
- Minty B.R.S. 1997. Fundamentals of airborne gamma-ray spectrometry. *Journal of Australian Geology & Geophysics*, 17 (2), 39-50. Available on line at: <http://pid.geoscience.gov.au/dataset/ga/81491> / (accessed on 27 April 2022)
- Murthy I.V.R. 1985. Magnetic interpretation of dike anomalies using derivatives. *Pure and Applied Geophysics*, 123, 232-238. <https://doi.org/10.1007/BF00877019>
- Nabighian M.N. 1972. The analytic signal of two-dimensional magnetic bodies with polygonal cross-section: its properties and use for automated anomaly interpretation. *Geophysics*, 37(3), 507-517. <http://dx.doi.org/10.1190/1.1440276>
- Nabighian M.N. 1974. Additional comments on the analytic signal of two dimensional magnetic bodies with polygonal cross-section: *Geophysics*, 39, 85-92. <http://dx.doi.org/10.1190/1.1440416>
- Nabighian M.N. 1984. Toward a three-dimensional automatic interpretation of potential field data via generalized Hilbert transforms: Fundamental relation *Geophysics*, 49, 957-966. <https://doi.org/10.1190/1.1441706>
- Nunes N.S.V. 2000. Geologia e resultados prospectivos das áreas Morro do Leme e Morro Sem Boné/Mato Grosso. Goiânia: CPRM. (Informe de Recursos Minerais. Série Metais do Grupo da Platina e Associados, n. 19). Available on line at: <https://rigeo.cprm.gov.br/handle/doc/1615> / (accessed on 27 April 2022)
- Oliveira C.E.S., Prado E.M.G., Silva G.F., Graça M.C. 2015. Carta geofísica-geológica do Bloco Sudeste: áreas Rondônia e Acre. Projeto Províncias Metalogenéticas do Brasil. Porto Velho: CPRM. Escala 1:250.000. Available on line at: <https://rigeo.cprm.gov.br/handle/doc/21611> / (accessed on 27 April 2022)
- Phillips J.D. 2000. Locating magnetic contacts: a comparison of the horizontal gradient, analytic signal, and local wavenumber methods. In: Annual International Meeting, 70, 402-405. <https://doi.org/10.1190/1.1816078>
- Pimentel M. M., Fuck R.A. 1992. Neoproterozoic crustal accretion in Central Brazil. *Geology*, 20(4), 375-379. [https://doi.org/10.1130/0091-7613\(1992\)020<0375:NCAICB>2.3.CO;2](https://doi.org/10.1130/0091-7613(1992)020<0375:NCAICB>2.3.CO;2)
- Pinto Filho F.P., Freitas A.F., Melo C.F., Romanini S.J. 1977. Projeto Sudeste de Rondônia. Porto Velho: CPRM. v. 1. Available on line at: <https://rigeo.cprm.gov.br/handle/doc/9591> / (accessed on 27 April 2022)
- Pratt D.A., Shi Z. 2004. An Improved Pseudo-gravity Magnetic Transform Technique for Investigation of Deep Magnetic Source Rocks. In: Geophysical Conference and Exhibition, 17. <https://doi.org/10.1071/ASEG2004ab116>
- Priem H.N.A., Bon E.H., Verdurmen E.A.T., Bettencourt J.S. 1989. Rb-Sr chronology of Precambrian crustal evolution in Rondônia (western margin of the Amazonian craton). *Journal of South American Earth Sciences*, 2(2), 163-170. [https://doi.org/10.1016/0895-9811\(89\)90044-8](https://doi.org/10.1016/0895-9811(89)90044-8)
- Quadros M.L.E.S.; Rizzotto G.J. 2007. Geologia e recursos minerais do Estado de Rondônia: texto explicativo do mapa geológico e de recursos minerais do Estado de Rondônia. Porto Velho: CPRM. 116 p. Escala 1:1.000.000. Available on line at: <https://rigeo.cprm.gov.br/handle/doc/10277> / (accessed on 27 April 2022)
- Rao D.A., Babu H.V., Narayan P.V. 1981. Interpretation of magnetic anomalies due to dikes: The complex gradient method. *Geophysics*, 46, 1572-1578. <https://doi.org/10.1190/1.1441164>
- Reeves C. 2005. Aeromagnetic surveys: principles, practice and interpretation. Delft, Geosoft, 155 p.
- Rizzotto G. J. (org.). 2010. Geologia e recursos minerais da Folha Pimenteiras SD.20-X-D: texto explicativo do mapa geológico e de recursos minerais da Folha Pimenteiras. Porto Velho, CPRM, 136 p. Escala 1:250.000. Available on line at: <https://rigeo.cprm.gov.br/handle/doc/10908> / (accessed on 27 April 2022)
- Rizzotto G. J. 2014. Geologia e recursos minerais da Folha Vilhena (SD.20-X-B): texto explicativo do mapa geológico e de recursos minerais da Folha Vilhena. Porto Velho, CPRM, 175. Escala 1:250.000. Available on line at: <https://rigeo.cprm.gov.br/handle/doc/17473> / (accessed on 27 April 2022)
- Rizzotto G.J., Bettencourt J.S., Teixeira W., Pacca I.I.G., D'Agrella M.S., Vasconcelos P., Basei M.A.S. 2002. Geologia e geocronologia da Suíte Metamórfica Colorado e suas encaixantes, SE de Rondônia: implicações para a evolução mesoproterozóica do SW do Cráton

- Amazônico. *Geologia USP, Série Científica* 2, 41–55. <https://doi.org/10.5327/S1519-874X2002000100006>
- Rizzotto G.J., Hartmann L.A. 2012. Geological and geochemical evolution of the Trincheira Complex, a Mesoproterozoic ophiolite in the southwestern Amazon Craton, Brazil. *Lithos*, 148, 277–295. <https://doi.org/10.1016/j.lithos.2012.05.027>
- Rizzotto G.J., Santos J.O.S., Hartmann L.A., Tohver E., Pimentel M.M., McNaughton N.J. 2013. The Mesoproterozoic Guaporé suture in the SW Amazonian Craton: geotectonic implications based on field geology, zircon geochronology and Nd-Sr isotope geochemistry. *Journal of South American Earth Sciences*, 48, p. 271–295. <https://doi.org/10.1016/j.jsames.2013.10.001>
- Roest W.R., Verhoef J., Pilkington M. 1992. Magnetic interpretation using the 3-D analytic signal. *Geophysics*, 57(1), 116–125. <http://dx.doi.org/10.1190/1.1443174>
- Romanini S.J. 1997. Mapa geológico preliminar da Serra Céu Azul/RO: prospecção geoquímica e síntese geológico-metalogenética. Porto Alegre, CPRM. (Informe de Recursos Minerais. Série Metais do Grupo da Platina e Associados, 03). Available on line at: <https://rigeo.cprm.gov.br/handle/doc/1598> / (accessed on 27 April 2022)
- Romanini S.J. 2000. Geologia e prospecção geoquímica/aluvionar da área Corumbiara / Chupinguaia-Rondônia. Porto Alegre, CPRM. (Informe de Recursos Minerais. Série Metais do Grupo da Platina e Associados, 06). Available on line at: <https://rigeo.cprm.gov.br/handle/doc/1601> / (accessed on 27 April 2022)
- Ruiz A.S. 2005. Evolução geológica do sudoeste do Cráton Amazônico, região limítrofe Brasil-Bolívia, Mato Grosso. Universidade Estadual de São Paulo, Rio Claro, São Paulo, Brazil.
- Saes G.S., Cesar A.R.S.F. 1996. Acreção de terrenos mesoproterozóicos no SW da Amazônia. In: Congresso Brasileiro de Geologia, 39, 1, 348. Available on line at: <http://www.sbgeo.org.br/home/pages/44#Anais%20de%20Congressos%20Brasileiros%20de%20Geologia> / (accessed on 27 April 2022)
- Salem A., Williams S., Fairhead D., Smith R., Ravat D. 2007. Interpretation of magnetic data using tilt-angle derivatives. *Geophysics*, 73(1), L1-L10. <https://doi.org/10.1190/1.2799992>
- Santos J.O.S., Hartmann L.A., Gaudette H.E., Groves D.I., McNaughton N., Fletcher I.R. 2000. A new understanding of the provinces of the Amazon Craton based on integration of field mapping and U-Pb and Sm-Nd geochronology. *Gondwana Research* 3(4), 453–488. [https://doi.org/10.1016/S1342-937X\(05\)70755-3](https://doi.org/10.1016/S1342-937X(05)70755-3)
- Scandolara J.E. 2006. Geologia e evolução do terreno Jamari, embasamento da faixa Sunsás/Aguapei, centro-leste de Rondônia, sudoeste do Cráton Amazônico. PhD Thesis, Universidade de Brasília, Brasília, 457 p. Available on line at: <https://repositorio.unb.br/handle/10482/2498> / (accessed on 27 April 2022)
- Scandolara J.E., Amorim J.L. 1999. A faixa móvel Guaporé, sua definição e inserção no contexto geotectônico do SW do Cráton Amazônico. In: Simposium Nacional de Estudos Tectônicos, 6, 24–27.
- Scandolara J.E., Rizzotto G.J., Bahia R.B.C., Quadros M.L.E.S., Amorim J.L., Dall'Igna L.G. 1999. Geologia e Recursos Minerais do Estado de Rondônia: texto explicativo e mapa geológico na escala 1:1.000.000. Brasília, CPRM. Available on line at: <https://rigeo.cprm.gov.br/handle/doc/10277> / (accessed on 27 April 2022)
- Schobbenhaus C. 2001. Geological map of South America. Brasília, CPRM; DNPM; UNESCO. Escala 1:5.000.000. Available on line at: <https://rigeo.cprm.gov.br/handle/doc/2542> / (accessed on 27 April 2022)
- Stewart J.R., Betts P.G. 2010. Implications for Proterozoic plate margin evolution from geophysical analysis and crustal-scale modeling within the western Gawler Craton, Australia. *Tectonophysics*, 483, 151–177. <https://doi.org/10.1016/j.tecto.2009.11.016>
- Tassinari C.C.G. 1981. Evolução geotectônica da província Rio Negro-Juruema na região Amazônica. MSc Dissertation, Instituto de Geociências, Universidade de São Paulo, São Paulo, 2 v. DOI: [10.11606/D.44.1981.tde-11062013-163626](https://doi.org/10.11606/D.44.1981.tde-11062013-163626)
- Tassinari C.C.G., Bettencourt J.S., Geraldes M.C., Macambira M.J.B., Lafon J.M. 2000. The Amazonian Craton. In: Cordani U.G., Milani E.J., Thomaz Filho A., Campos D.A. (ed.). *Tectonic evolution of South America*. Rio de Janeiro, Brazil, 31st International Geological Congress, p. 41–95. Available on line at: http://www.cprm.gov.br/publique/media/recursos_minerais/livro_1_147.pdf / (accessed on 27 April 2022)
- Tassinari C.C.G., Cordani, U.G., Nutman, A.P., Van Schmus, W.R., Bettencourt, J.S., Taylor, P.N., 1996. Geochronological systematics on basement rocks from the Rio Negro-Juruena Province (Amazonian Craton) and tectonic implications. *International Geology Review* 38, 161–175. <https://doi.org/10.1080/00206819709465329>
- Tassinari C.C.G., Macambira M.J.B. 1999. Geochronological provinces of the Amazonian Craton. *Episodes*, 22, 174–182. <https://doi.org/10.18814/epiiugs/1999/v22i3/004>
- Tassinari C.C.G., Siga Jr. O., Teixeira W. 1984. Épocas metalogenéticas relacionadas à granitogênese do Cráton Amazônico. In: Congresso Brasileiro de Geologia, 33, v. 6., 2963–2977. Available on line at: <http://www.sbgeo.org.br/home/pages/44#Anais%20de%20Congressos%20Brasileiros%20de%20Geologia> / (accessed on 27 April 2022)
- Teixeira W., Tassinari C.C.G. 1984. Caracterização geocronológica da Província Rondoniana e suas implicações geotectônicas. In: *Symposium Amazônico*, 2, p. 75–86.
- Teixeira W., Tassinari C.C.G., Cordani U.G., Kawashita K. 1989. A review of the geochronology of the Amazonian Craton: tectonic implications. *Precambrian Research*, 42, 213–227. [https://doi.org/10.1016/0301-9268\(89\)90012-0](https://doi.org/10.1016/0301-9268(89)90012-0)
- Thompson D.T. 1982. EULDPH: A new technique for making computer-assisted depth estimates from magnetic data. *Geophysics*, 47, 31–37. <https://doi.org/10.1190/1.1441278>
- Tohver E., D'Agrella-Filho M.S., Trindade R.I.F. 2006. Paleomagnetic record of Africa and South America for the 1200–500Ma interval, and evaluation of Rodinia and Gondwana assemblies. *Precambrian Research*, 47(3–4), 193–222. <https://doi.org/10.1016/j.precamres.2006.01.015>
- Tohver E., Van der Pluijm, B.A.; Mezger, K.; Scandolara, J.E.; Essene, E J. 2005. Two stage tectonic history of the SW Amazon craton in the late Mesoproterozoic: identifying a cryptic suture zone. *Precambrian Research*, 137, 35–59, 2005. <https://doi.org/10.1016/j.precamres.2005.01.002>
- Verduzco B., Fairhead J.D., Green C.M., MacKenzie C. 2004. New insights into magnetic derivatives for structural mapping. *The Leading Edge*, 23(2), 116–119. <https://doi.org/10.1190/1.1651454>
- Wilford J.R., Bierwirth P.N., Craig M.A. 1997. Application of airborne gamma-ray spectrometry in soil/regolith mapping and applied geomorphology. *AGSO Journal of Australian Geology & Geophysics*, 17(2), 201–206. Available on line at: <http://pid.geoscience.gov.au/dataset/ga/81503> / (accessed on 27 April 2022)